sequentially to the onset frame (immediately prior to which there were no facial movements). And from the onset, we moved the video forward sequentially to the offset (immediately following which there were no facial movements).

1.4. Coding

Two coders independently identified spontaneous smiles and laughs using the Digital Video Camera Recorder (SONY DCR-PC110). Only spontaneous smiles and laughs identified by both coders were included in the subsequent analysis. The percentage of intercoder agreement was 91.67%. Correlation of the event durations recorded by the two coders was $r=0.92$ ($p<0.01$).

2. Results

2.1. Spontaneous smiles in Group A

Twenty-four spontaneous smiles were observed (the frequency range per newborn was 1 to 6). The durations of spontaneous smiles were determined by averaging the durations recorded by the two coders. The mean duration was 1.97 s (S.D. = 0.68). An analysis of duration found no gender difference (female: 1.94 s, male: 1.99 s), no Apgar score effect (Apgar 9: 2.00 s, Apgar 8: 1.93 s), no gestational age effect (37–38 weeks: 2.00 s, 39–40 weeks: 1.93 s), and no age effect (2 to 4 days old: 1.95 s, 5 to 8 days old: 1.98 s).

Unilateral spontaneous smiles were more frequently observed than bilateral spontaneous smiles (unilateral: 20, bilateral: 4), $\chi^2(1)=10.6$, $p<0.01$. An example of a unilateral smile from an infant in Group B is shown in Fig. 1. When lying on one side, unilateral spontaneous smiles were more frequently observed on the side of the face away from the surface of the bed (top side: 18, bottom side: 2), $\chi^2(1)=12.8$, $p<0.01$, as in Fig. 1, where the infant is lying on his right side and smiling on his left side. Unilateral spontaneous smiles were more frequently observed on the left side of the face than the right side (left: 13, right: 7), although this difference was not statistically significant.

2.2. Spontaneous smiles in Group B

The mean duration of observations was 174.15 min (S.D. = 130.06) per infant. There were 82 spontaneous smiles observed, 21 in newborns less than 1 month old, 41 in infants 1 month old, and 20 in those 2 months old.

Of the 24 spontaneous smiles observed in mothers' arms, 5 were on the right side of the face, 4 were on the left side, and 15 were bilateral.

Of the 58 spontaneous smiles observed in infants lying on beds, the laterality of 5 could not be determined. Fig. 2, depicting a 42-day-old infant, shows how a smile can change from unilateral to bilateral. The laterality of this smile could not be determined. Among 53 spontaneous smiles, bilateral smiles were more frequent than unilateral smiles (bilateral: 36, unilateral: 17), $\chi^2(1)=6.8$, $p<0.01$. Unilateral spontaneous smiles were more frequent on the side away from the bed surface (side away from bed: 16, side near bed: 1), $\chi^2(1)=13.2$, $p<0.01$. There was no statistically significant difference in frequency of unilateral smiles on different sides of the face (left: 10, right: 7).

Figure 2 Spontaneous smile changes from unilateral to bilateral.

3. Spontaneous smiles in Groups A and B

Combining the data from Groups A and B, Fig. 3A shows the percentage of bilateral smiles in different aged infants

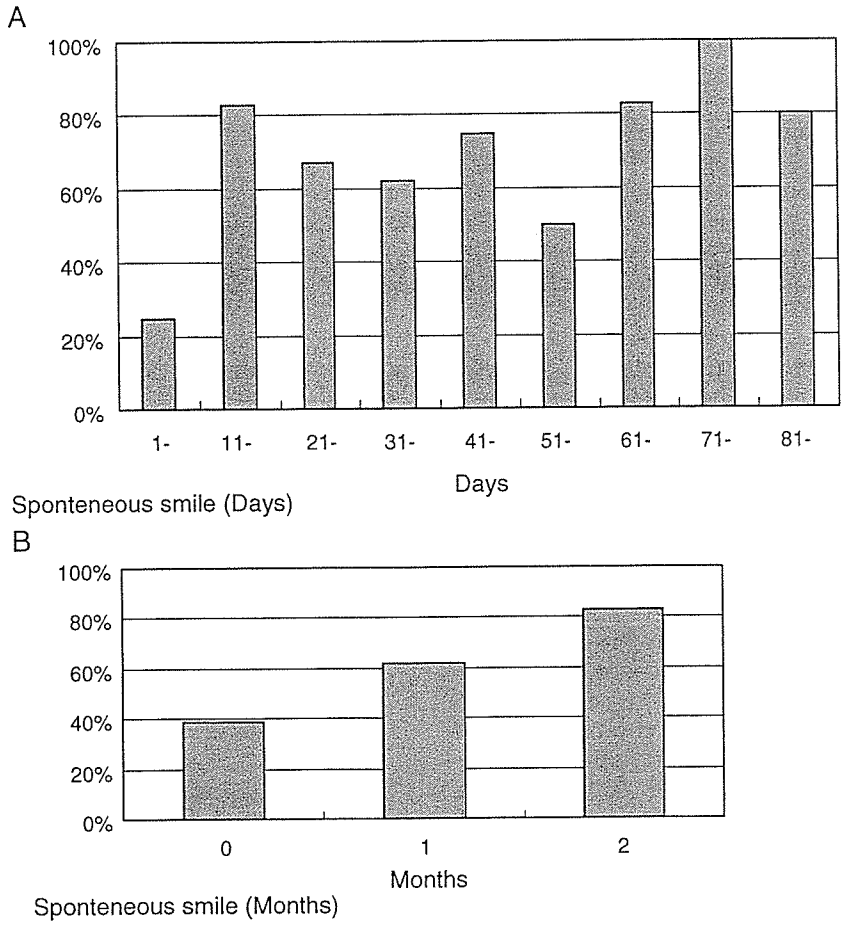

Figure 3 (A) Percentages of bilateral spontaneous smile by 10 days. (B) Percentages of bilateral spontaneous smile by month.

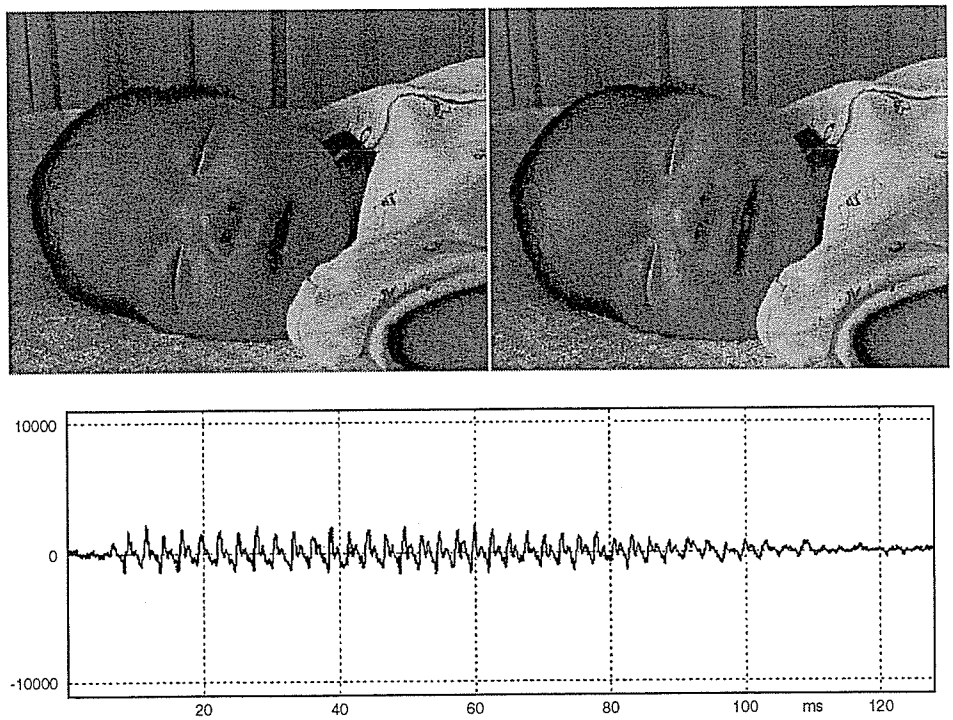

Figure 4 Spontaneous laugh. Abscissa indicates millisecond, and ordinate amplitude.

(grouped in 10-day periods). Fig. 3-2 shows the same data grouped by month. These figures show that the proportion of bilateral smiles increases gradually and consistently with age.

Unilateral spontaneous smiles occurred more frequently on the side of the face away from the bed surface (side away from bed: 34, side near bed: 3), $\chi^2(1)=26.0$, $p<0.01$.

The frequency of unilateral smiles did not significantly differ on the right and left sides of the face when the infant was being held by the mother (right: 5, left: 4). However, there were significant differences when the infant was lying on a bed (right: 14, left: 23), $\chi^2(1)=6.0$, $p<0.05$.

3.1. Spontaneous laugh in Group B

As noted in the METHOD section, spontaneous laughs are different from spontaneous smiles only because they involve vocal laughing sounds. Nine spontaneous laughs were observed. Three out of the four infants who were observed from 0 months of age showed spontaneous laughter—one 17-day-old female, one 24-day-old male, and another 26-day-old male. Fig. 4 shows facial changes and sound waves of the 26-day-old while spontaneously laughing. One female showed 4 spontaneous laughs when 1 to 2 months of age. The mean duration of facial changes during spontaneous laughter was 3.08 s. The mean duration of spontaneous laughs was longer than that of spontaneous smiles (2.17 s), $F(1,113)=7.75$, $p<0.01$. All spontaneous laughs were bilateral.

4. Discussion

Holowka and Petitto [12], using infants from 5 to 12 months, showed that babies open the right side of their mouth while babbling, and open the left side while smiling. They claimed that left hemisphere cerebral specialization while babbling suggests language functions in humans are lateralized from a very early point in development. And they thought that babies' emotional expression may be controlled by the right hemisphere even at the early age of 5 months. Our results on spontaneous smiling in Group A support the early stage of their hypothesis, but as we saw in the data of Group B, the dominance of unilateral spontaneous smiling disappears later. We speculate that this may be one of the U-shaped phenomena in developmental psychology described by Siegler [13].

We found dominance of unilateral spontaneous smiles on the side of the face away from the surface of the bed and on the left side of the face. Can we relate unilateral smiles to the asymmetrical tonic neck reflex (ATNR: [14]) in newborn infants? ATNR is observed during the first 2 or 3 months of life, and it is usually gone by 6 or 7 months [14]. When the participants showed the bilateral spontaneous smiles, they were more likely to be laying on their right side than their left (right: 25, left: 7), $\chi^2(1)=10.2$, $p<0.01$. When showing unilateral spontaneous smiles, they were more likely to be laying on their right side than their left side (right: 26, left 11), $\chi^2(1)=6.0$, $p<0.05$. The dominance of unilateral spontaneous smiles on left side of the face may be related to the ATNR.

Fig. 3A shows there is a large increase in smiles after 10 days and, possibly, another increase after 51 days. This hints at the possibility that a more conscious, less sleep-linked smile is developing or 'coming on-line'.

The rise of bilateral smiling suggests the development of a more mature behavioral pattern and perhaps the development of more mature cerebral control over these behaviors. The longer duration of laughter and increased number of bilateral smiles over a period of days suggest that these are more stable behavioral structures than unilateral smiles.

Sroufe and Waters [15] thought "laughter" appears at about 4 months. How can we explain this discrepancy? Might this be further evidence of the U-shaped phenomenon? The durations of spontaneous laughs were longer than those of spontaneous smiles, but the frequency of laughs was much lower. "Spontaneous smile" and "Spontaneous laugh" might be different behaviors from the beginning.

To record spontaneous smiles and laughs in more detail, it will be necessary to observe them by more intensive longitudinal research designs.

Acknowledgements

We would like to thank Mary Blish, John C. Nesbit, Naoe Masuda, and Fumito Kawakami for their kind support. And we wish to express our appreciation to the infants and their parents for their help and the many important comments by the reviewers.

References

[1] Wolff P. Observations on newborn infants. Psychosom Med 1959;21:110-8.
[2] Wolff P. Observations on the early development of smiling. Foss BM, editor. Determinants of infant behavior, vol. 2. London: Methuen; 1961. p. 113-38.
[3] Emde RN, McCartney RD, Harmon RJ. Neonatal smiling in rem states: IV. Premature study. Child Dev 1971;42:1657-61.
[4] Freedman D. Hereditary control of early social behavior. Foss BM, editor. Determinants of infant behavior, vol. 3. London: Methuen; 1965. p. 149-59.
[5] Freedman D. Human infancy: an evolutionary perspective. Hillsdale: LEA; 1974.
[6] Gewirtz JL. The course of infant smiling in four child-rearing environments in Israel. Foss BM, editor. Determinants of infant behavior, vol. 3. London: Methuen; 1965. p. 205-48.
[7] Shimada S. The development of smiling response in early infancy (in Japanese). Seishinshinkeigaku-zashi (J Psychoneurology) 1969;71:741-56.
[8] Messinger D, Dondi M, Nelson-Goens GC, Beghi A, Fogel F, Simion F. How sleeping neonates smile. Dev Sci 2002;5:48-54.
[9] Oster H. Facial expression and affect development. In: Lewis M, Rosenblum LA, editors. The development of affect. New York: Plenum Press; 1978. p. 43-74.
[10] Ekman P, Friesen W. http://www-2.cs.cmu.edu/afs/cs/project/face/www/facs.htm 1978.

[11] Izard CE. The maximally discriminative facial movement coding system. Instructional Resources Center, University of Delaware;1983.
[12] Holowka S, Petitto LA. Left hemisphere cerebral specialization for babies while babbling. Science 2002;297:1515.
[13] Siegler RS. U-shaped interest in u-shaped development—and what it means. J Cogn Dev 2004;5:1-10.
[14] Snow CW. Infant development. Englewood Cliffs: Prentice Hall; 1989.
[15] Sroufe LA, Waters E. The ontogenesis of smiling and laughter: a perspective on the organization of development in infancy. Psychol Rev 1976;83:173-89.

Cellular/Molecular

An Analog of a Dipeptide-Like Structure of FK506 Increases Glial Cell Line-Derived Neurotrophic Factor Expression through cAMP Response Element-Binding Protein Activated by Heat Shock Protein 90/Akt Signaling Pathway

Xiaobo Cen,[1,2*] Atsumi Nitta,[1*] Shin Ohya,[1] Yinglan Zhao,[1] Naoya Ozawa,[1] Akihiro Mouri,[1] Daisuke Ibi,[1,7] Li Wang,[2] Makiko Suzuki,[3] Kuniaki Saito,[3] Yasutomo Ito,[4] Tetsuya Kawagoe,[5] Yukihiro Noda,[1,6] Yoshihisa Ito,[1,7] Shoei Furukawa,[8] and Toshitaka Nabeshima[1]

[1]Department of Neuropsychopharmacology and Hospital Pharmacy, Nagoya University Graduate School of Medicine, Nagoya 466-8560, Japan, [2]National Chengdu Center for Safety Evaluation of Traditional Chinese Medicine, West China Hospital, Sichuan University, Chengdu 610041, China, [3]Department of Laboratory Medicine, Gifu University School of Medicine, Gifu 500-8705, Japan, [4]Equipment Center for Research and Education, Nagoya University Graduate School of Medicine, Nagoya 466-8560, Japan, [5]Department of Research and Development, Initium, Tokyo, 107-0062, Japan, [6]Division of Clinical Science in Clinical Pharmacy Practice, Management and Research, Faculty of Pharmacy, Meijo University, Nagoya 468-8503, Japan, [7]Department of Pharmacology, College of Pharmacy, Nihon University, Funabashi-shi, Chiba 274-8555, Japan, and [8]Laboratory of Molecular Biology, Gifu Pharmaceutical University, Gifu 502-8585, Japan

Glial cell line-derived neurotrophic factor (GDNF) is an important neurotrophic factor that has therapeutic implications for neurodegenerative disorders. We previously showed that leucine-isoleucine (Leu-Ile), an analog of a dipeptide-like structure of FK506 (tacrolimus), induces GDNF expression both *in vivo* and *in vitro*. In this investigation, we sought to clarify the cellular mechanisms underlying the GDNF-inducing effect of this dipeptide. Leu-Ile transport was investigated using fluorescein isothiocyanate-Leu-Ile in cultured neurons, and the results showed the transmembrane mobility of this dipeptide. By liquid chromatography-mass spectrometry and quartz crystal microbalance assay, we identified heat shock cognate protein 70 as a protein binding specifically to Leu-Ile, and molecular modeling showed that the ATPase domain is the predicted binding site. Leu-Ile stimulated Akt phosphorylation, which was attenuated significantly by heat shock protein 90 (Hsp90) inhibitor geldanamycin (GA). Moreover, enhanced interaction between phosphorylated Akt and Hsp90 was detected by immunoprecipitation. Leu-Ile elicited an increase in cAMP response element binding protein (CREB) phosphorylation, which was inhibited by GA, indicating that CREB is a downstream target of Hsp90/Akt signaling. Leu-Ile elevated the levels of GDNF mRNA and protein expression, whereas inhibition of CREB blocked such effects. Leu-Ile promoted the binding activity of phosphorylated CREB with cAMP response element. These findings show that CREB plays a key role in transcriptional regulation of GDNF expression induced by Leu-Ile. In conclusion, Leu-Ile activates Hsp90/Akt/CREB signaling, which contributes to the upregulation of GDNF expression. It may represent a novel lead compound for the treatment of dopaminergic neurons or motoneuron diseases.

Key words: GDNF; dipeptide; FK506; Hsp90; Hsc70; CREB

Introduction

Glial cell line-derived neurotrophic factor (GDNF) is an important neurotrophic factor that regulates the development, migration, and survival of neurons, and has therapeutic implications for neurodegenerative disorders (Airaksinen and Saarma, 2002). We have demonstrated that leucine-isoleucine (Leu-Ile), an analog of a dipeptide-like structure of FK506, shows nonimmunosuppressive activity and promotes neuronal survival through induction of GDNF in both *in vivo* and *in vitro* studies (Nitta et al., 2004), but the mechanism is unclear.

Studies have indicated the complex regulatory mechanisms of GDNF expression. It can be induced by diverse extracellular stimuli (Verity et al., 1999; Castro et al., 2005), and multiple transcription factor binding sites have been identified in the promoter sequence of the GDNF gene (Woodbury et al., 1998), such as cAMP response element (CRE) binding protein (CREB) (Matsushita et al., 1997; Baecker et al., 1999). Previous studies showed that CREB activation is associated with GDNF expression (Young

Received Aug. 6, 2005; revised Feb. 2, 2006; accepted Feb. 2, 2006.

This work was supported in part by a grant-in-aid for Science Research and Special Coordination Funds for Promoting Science and Technology, Target-Oriented Brain Science Research Program KAKENHI, and the 21st Century Center of Excellence Program "Integrated Molecular Medicine for Neuronal and Neoplastic Disorders" from the Ministry of Education, Culture, Sports, Science and Technology of Japan; by a grant-in-aid for Health Science Research on Regulatory Science of Pharmaceuticals and Medical Devices, and Dementia and Fracture from the Ministry of Health, Labor and Welfare of Japan; and by a Smoking Research Foundation grant for Biomedical Research.

*A.N. and X.C. contributed equally to this work.

Correspondence should be addressed to Toshitaka Nabeshima, Department of Neuropsychopharmacology and Hospital Pharmacy, Nagoya University Graduate School of Medicine, Tsuruma-Cho, Showa-ku, Nagoya 466-8560, Japan. E-mail: tnabeshi@med.nagoya-u.ac.jp.

DOI:10.1523/JNEUROSCI.5010-05.2006

 0270-6474/06/263335-10$15.00/0

et al., 1999; Lenhard et al., 2002), implying that CREB may participate in regulating GDNF expression as a transcriptional factor. Phosphorylation of CREB at serine-133 (Ser^{133}) within the kinase-inducible domain is critical for its function as a stimulus-dependent transcriptional activator, and multiple kinases have been implicated as activators of CREB in neurons, including protein kinase C (PKC) (Roberson et al.,1999), calmodulin kinase II (CaMKII) (Lee et al., 2004), extracellular signal-regulated kinase 1/2 (ERK1/2) (Schinelli et al., 2001), and serine/threonine kinase Akt (Brunet et al., 2001). Different extracellular stimuli may activate distinct signalings, which contribute to CREB phosphorylation and cellular responses. In particular, CREB is considered to be a regulatory target for Akt, and Akt can promote cell survival by stimulating the expression of cellular genes via the CREB-dependent pathway (Du and Montminy, 1998; Pugazhenthi et al., 2000).

Although phosphoinositide 3-kinase (PI3-k) is an important activator for Akt, increasing evidence has indicated that Akt can be regulated in PI3-k independent manners in neurons, such as ERK1/2 and CaMK cascades (Yano et al., 1998; Brami-Cherrier et al., 2002). Moreover, Akt is a well characterized heat shock protein 90 (Hsp90)-dependent kinase (Basso et al., 2002; Xu et al., 2003), and chaperones Hsp90 and heat shock cognate protein 70 (Hsc70) have been demonstrated to play a role in Akt regulation through distinct mechanisms. For instance, Hsp90–Akt interaction increases Akt activity by protecting it from dephosphorylation by protein phosphatase 2A (PP2A) (Sato et al., 2000; Yun and Matts, 2005); the binding of client molecule to Hsc70 maintains Akt phosphorylation and downstream cascade activation by inhibiting its proteasomal degradation based on Hsc70/Hsp90 machinery (Doong et al., 2003). Therefore, modulation of Hsp90 resulting from a variety of physiological or pharmacological factors may alter Akt signaling, contributing to the regulation of cellular function and response (Pratt and Toft, 2003). It is known that Hsp90 ATPase activity is highly regulated by the binding of cochaperone or client proteins, such as FK506 binding protein (FKBP) and Hsc70 (McLaughlin et al., 2002).

We defined a signaling cascade in which Leu-Ile promotes CREB phosphorylation via Hsp90/Akt signaling, which plays an important role in the transcriptional regulation of the GDNF gene. Moreover, Hsc70 is likely to cooperate with Hsp90 as a cochaperone to modulate Akt activity.

Materials and Methods

Materials. Leu-Ile, proline-leucine (Pro-Leu), and isoleucine-proline (Ile-Pro) were synthesized by Kokusan Chemical (Tokyo, Japan). Leu-Ile labeled with fluorescein isothiocyanate (FITC) was prepared by Thermo Electron Corporation (Ulm, Germany). Geldanamycin (GA) and 2-(4-morpholinyl)-8-phenyl-1(4*H*)-benzopyran-4-one (LY294002) were purchased from Sigma (St. Louis, MO). FK506 was gifted from Fujisawa Pharmaceutical (Osaka, Japan). Anti-Hsp70, anti-Hsp90, anti-phosphorylated Akt (pAkt; Thr308), anti-Akt, anti-pCREB (Ser^{133}), anti-CREB, anti-ERK1/2, anti-pERK1/2 (Thr202/Tyr204), anti-pCaMKIIα,β, anti-phosphorylated p38 mitogen-activated protein kinase (pP38MAPK) (Thr180/Tyr182), anti-phosphorylated stress-activated protein kinase/Jun-terminal kinase (pSAPK/JNK) (Thr183/Tyr185), and anti-microtubule-associated protein 2 (MAP2) antibodies were purchased from Cell Signaling Technology (Beverly, MA). Anti-PKC, anti-c-Src, and anti-actin antibodies were from Santa Cruz Biotechnology (Santa Cruz, CA). Anti-Hsc70 antibody and recombinant Hsc70 were from Stressgen Biotechnologies (Victoria, Canada). Anti-GDNF antibody was from R&D Systems (Minneapolis, MN). Anti-glial fibrillary acidic protein (GFAP) antibody was from Chemicon International (Temecula, CA).

Primary hippocampal neuron cultures. Primary hippocampal neuronal cultures were prepared from day 17 embryos of rats. Briefly, hippocampi were dissected and digested with 0.25% trypsin at 37°C for 30 min. Hippocampal cells were plated in polyornithine-coated plates in DMEM/F12 medium containing 10% fetal bovine serum. The medium was replaced with DMEM/F12 medium containing 1% N2 supplement (Invitrogen, San Diego, CA) 24 h later. MAP2-positive cells accounted for over 95% of the total in cultures.

Transmembrane transport of Leu-Ile. Cultured neurons were incubated with FITC-Leu-Ile or FITC at various concentrations for the indicated periods at 37°C. Cells were washed three times with PBS and collected in 300 μl PBS using a rubber scratcher. After samples were sonicated and centrifuged at 10,000 × *g* for 30 min at 4°C, the supernants (200 μl) were collected for fluorescent density measurement at an excitation wavelength of 485 nm and an emission wavelength of 518 nm by Fluoroskan Ascent (Thermo Labsystems, Waltham, MA). The intracellular amount of FITC-Leu-Ile or FITC was calculated according to the standard curve.

Identification of binding protein for Leu-Ile in mouse brain. Brains were removed from 7-week-old male Institute of Cancer Research mice (Nippon SLC, Shizuoka, Japan), and homogenized in radioimmunoprecipitation assay (RIPA) buffer (20 mM Tris-HCl, pH7.4, 0.25 M NaCl, 5 mM EDTA, 1% Triton X-100, 1 mM PMSF, and 1 μg/ml each of leupeptin, aprotinin, and pepstatin A). After centrifugation at 10,000 × *g* for 60 min at 4°C, the supernants were collected and reacted with FITC-Leu-Ile for 60 min at 37°C. Samples from the reaction complex were subjected to gel electrophoresis, and the gels were analyzed directly by FluorImager595 (Molecular Dynamics, Sunnyvale, CA).

Preparation of Sepharose Affigel-10 (Amersham Biosciences, Arlington Heights, IL) coupled with Leu-Ile was performed according to manufacturer's instructions. The column with Affigel-10 coupled with Leu-Ile was loaded with brain homogenates and equilibrated with 10 mM Tris-HCl buffer, pH 7.4, at 4°C overnight. The column was washed extensively with 0.1 M PBS, pH 7.4, followed by elution with 0.17 M glycine-HCl buffer, pH 3.0. The eluants were separated by gel electrophoresis. To identify the binding protein by liquid chromatography-mass spectrometry (LC-MS), the specific protein band was excised from the gel after silver staining and digested in-gel with trypsin. The digested peptide fragments were directly sprayed into a Q-Tof hybrid mass spectrometer equipped with an electrospray source (Q-Tof 2; Micromass, Manchester, UK). The analysis was conducted using Mascot Search (Matrix Science, Boston, MA) with reference to the protein sequence database at the National Center for Biotechnology Information (NCBI) (http://www.ncbi.nlm.nih.gov/Entrez). To validate the binding protein, samples from the reaction complex of brain homogenates with Leu-Ile were subjected to gel electrophoresis and then immunoblotted with anti-Hsc70 antibody. In addition, recombinant Hsc70 protein was reacted with Leu-Ile at 37°C for 60 min, and the reaction complex was separated by gel electrophoresis followed by Coomassie brilliant blue (CBB) staining.

Leu-Ile- or FK506-conjugated Affigel-10 was incubated with brain homogenates at 4°C overnight. The columns were washed extensively followed by elution with 0.17 M glycine-HCl buffer, pH 3.0. The eluants were separated by SDS-PAGE and immunoblotted with anti-Hsc70 antibody.

Interaction between Leu-Ile and Hsc70. The binding of Leu-Ile or FK506 for Hsc70 was examined by quartz crystal microbalance (QCM), which is useful for studying mass-measuring and molecular interaction in aqueous solutions (Motomiya et al., 2003). Briefly, 100 μl of each dipeptide (10 μg/ml in PBS) or FK506 [10 μg/ml in chloroform or chloroform/ethanol (1:1)] was immobilized into a QCM plate for 1 h at room temperature, and then removed. After washing three times with PBS, the plates were soaked in PBS at 25°C. Hsc70 or heat-denatured Hsc70 was applied to the equilibrated solution, and the change in resonance frequency was recorded using AFFINIX Q User Analysis software (AQUA; Initium, Tokyo, Japan). The binding affinity was indicated by frequency changes of QCM, and disassociation constant (K_d) was calculated with the AQUA software.

Modeling of functional domains of Hsc70 and the predicted binding site for Leu-Ile. To further understand the interaction between Hsc70 and Leu-Ile, molecular models of the ATPase domain, substrate-binding domain, and C-terminal domain of Hsc70 were generated using the three-

dimensional structural data from the Protein Data Bank (http://pdbbeta.rcsb.org/pdb/Welcome.do) in the Research Collaboratory for Structural Bioinformatics (Flaherty et al., 1990; Morshauser et al., 1999; Chou et al., 2003). Interaction of each domain with Leu-Ile was analyzed using Molecular Operating Environment (MOE) software (Chemical Computing Group, Montreal, Quebec, Canada). All calculations used an MMFF94x force field and a cutoff distance of 9.5 Å for nonbinding interactions. The Alpha Site Finder of the MOE program was used for docking stimulation.

Western blotting. Cultured neurons were lysed in RIPA buffer (20 mM Tris-HCl, pH 7.6, 150 mM NaCl, 1 mM sodium orthovanadate, 2 mM EDTA, 50 mM NaF, 1% Nonidet P-40, 1 mM PMSF, and 2 μg/ml each of aprotinin, leupeptin, and pepstatin). Lysates were sonicated and centrifuged at 9000 × *g* for 15 min. Protein concentrations were determined by protein assay reagents (Bio-Rad, Hercules, CA). The samples were subjected to SDS-PAGE and then electrotransferred to polyvinylidene difluoride membranes. The membranes were immunoblotted and developed using chemiluminescence detection reagents. To calculate the amount of phosphorylated form versus total protein, the same membranes were stripped, incubated with the primary antibody for total protein, and examined as described above. The relative amount of immunoreactive protein in each band was assayed by scanning densitometric analysis using the Atto Densitograph 4.1 system (Atto, Tokyo, Japan).

Immunoprecipitation. After centrifugation, the supernatants of cell lysates were normalized for protein concentration. A fraction (500 μg) of the total protein was incubated by gently rocking at 4°C overnight in the presence of anti-Hsp90 antibody. The immunocomplexes were captured by protein A Sepharose (Amersham Biosciences), washed out by lysis buffer, and then subjected to SDS-PAGE and immunoblotting.

Immunostaining. Cultured neurons attached to glass coverslips were fixed with 4% paraformaldehyde in PBS for 20 min, and then blocked in 3% normal serum and 0.1% Triton X-100 for 1 h. The coverslips were incubated with the primary antibodies at 4°C overnight, washed with PBS, and then incubated with appropriate secondary antibodies (Invitrogen) for 2 h. After being washed and mounted, stained neurons were observed under a fluorescent microscope (Axioscop 2 plus; Zeiss, Thornwood, NY).

Real-time RT-PCR. The level of GDNF mRNA was determined by real-time reverse transcription (RT)-PCR using an iCycler system (Bio-Rad). Briefly, isolation of total RNA was performed using RNeasy mini kit (Qiagen, Hilden, Germany). For reverse transcription, 1 μg RNA was converted into a cDNA by a standard 20 μl reverse transcriptase reaction using oligo-dT primers and Superscript II RT (Invitrogen). Total cDNA (1 μl) was amplified in a 25 μl reaction mixture using 0.1 μM each of forward and reverse primers and Platinum Quantitative PCR SuperMix-UDG (Invitrogen). Ribosomal mRNA was used and determined as the control for RNA integrity with TaqMan Ribosomal RNA control reagents (Applied Biosystems, Foster City, CA). The primer and dye probes were designed by Nippon Gene (Tokyo, Japan) using Primer Express software. The GDNF forward was 5′-AGCTGCCAGCCCAGAGAATT-3′ (base pair 288–307), with the reverse being 5′-GCACCCCCGATTTTTGC-3′ (base pair 354–370) and the dye probe being 5′-CAGAGGGAAAGGTCGCAGAGGCC-3′ (base pair 309–331).

Antisense oligonucleotide of CREB. CREB expression was inhibited by an oligodeoxynucleotide (ODN) targeting the initiation codon of CREB mRNA as previously reported (Johnson et al., 2000; Saini et al., 2004). The phosphorothioate ODNs were synthesized by Nisshinbo Industries (Tokyo, Japan). The sequence of antisense ODN was 5′-GCTCCAGAGTCCATGGTCAT-3′, with a sense ODN with the sequence 5′-ATGACCATGGACTCTGGAGC-3′ as a control. Transfections were performed using Lipofectamine reagent (Invitrogen), and oligonucleotide was added to culture medium at a final concentration of 4 μM. The inhibition of CREB expression after transfection was assessed by Western blotting. To investigate the role of CREB in transcriptional regulation of GDNF expression, cultures were incubated with CREB ODN before Leu-Ile treatment.

pCREB-CRE binding activity. Cultured neurons were collected and nuclear extracts were prepared by using BD TransFactor extraction kits (BD Biosciences, Franklin Lakes, NJ) according to the manufacturer's protocol. The CRE-pCREB binding activity was determined using

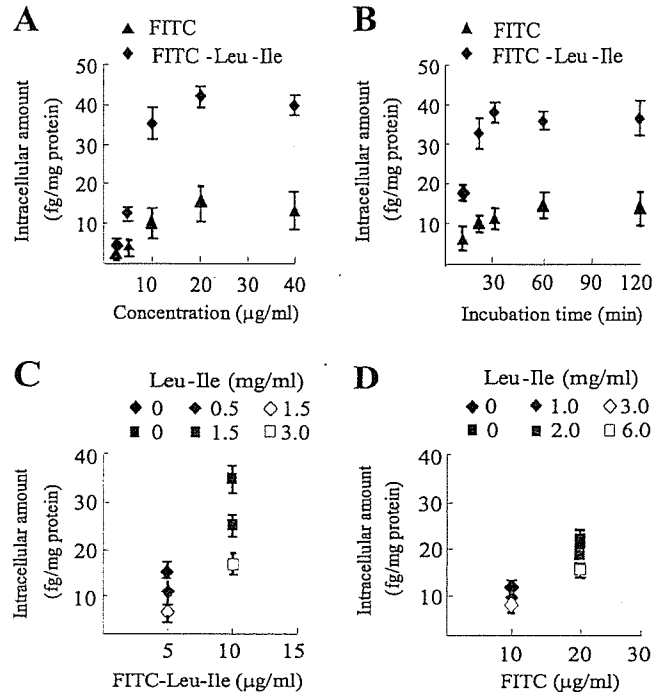

Figure 1. Transmembrane transport of Leu-Ile. ***A***, Cultured neurons were exposed to FITC-Leu-Ile or FITC at various concentrations for 30 min, and uptake was analyzed according to intracellular fluorescent densities ($n = 3$). ***B***, Neurons were incubated with 10 μg/ml FITC-Leu-Ile or FITC at 37°C for the indicated time periods. Time course uptake was analyzed ($n = 3$). ***C***, Neurons were exposed to FITC-Leu-Ile for 30 min in the presence of various concentrations of Leu-Ile, which were indicated by different symbols. Penetration of FITC-Leu-Ile was significantly inhibited by competitive Leu-Ile. ***D***, High concentrations of Leu-Ile could not inhibit FITC transport.

TransAM pCREB/CREB transcription factor assay kits (Active Motif Carlsbad, CA). Briefly, nuclear extract was applied to each well immobilized with oligonucleotide containing CRE 5′-TGACGTCA-3′, and incubated for 3 h. After washing, the wells were incubated with anti-pCREB antibody, followed by HRP-conjugated secondary antibody. After development with tetramethylbenzidine, the absorbance was measured with a microplate reader at 450 nm with reference at 655 nm. The specificity of the binding of pCREB to CRE was confirmed by conducting competitive experiments with 20 pmol of wild-type oligonucleotide probe or mutant probe containing the consensus CRE.

Statistical analysis. All data were expressed as means ± SEM. Statistical significance was determined by a one-way ANOVA, followed by the Student–Newman–Keuls test for multigroup comparisons. Differences were considered significant when $p < 0.05$.

Results

Transmembrane transport

As shown in Fig. 1*A*, uptake of FITC-Leu-Ile by neurons was increased with the elevation of extracellular concentration. Time-course studies showed that uptake of FITC-Leu-Ile by neurons was a quick process and appeared to be saturated after incubation for 60 min (Fig. 1*B*). Although transmembrane transport of FITC was observed in dose- and time-course studies, its penetration amount was much lower than that of FITC-Leu-Ile (Fig. 1*A*,*B*). Because specific inhibitor for neuronal peptide transporters is not available, competitive transport was investigated using high concentrations of Leu-Ile. Simultaneous incubation with various concentrations of Leu-Ile for 30 min significantly inhibited FITC-Leu-Ile transport in a concentration-dependent manner (Fig. 1*C*), but failed to inhibit FITC transport (Fig. 1*D*), suggesting that FITC-Leu-Ile and Leu-Ile are transported by the same

pathway. Together, these results strongly imply that FITC-Leu-Ile transport is mainly caused by the transmembrane activity of Leu-Ile rather than FITC and that the kinetics of FITC-Leu-Ile transport, at least in some degree, reflects that of Leu-Ile.

Identification of target protein for Leu-Ile in mouse brain

FITC-Leu-Ile was incubated with mouse brain homogenate, and the reaction complexes were subjected to electrophoresis. By fluorescent scanning, one specific fluorescent protein band with a molecular weight of ~70 kDa was detected, suggesting that this protein has the specific affinity for Leu-Ile (Fig. 2*A*, arrow). To further identify the protein binding to Leu-Ile, brain homogenate was applied to Leu-Ile-conjugated Affigel-10, and the eluants were subjected to electrophoresis and detected by silver staining. We found a specific protein band of ~70 kDa with stronger density in the gel (Fig. 2*B*, arrow), which was similar to that detected by fluorescent scanning. It has been known that the family of heat shock protein 70 represents an important cellular mechanism in neuroprotection (Rubio et al., 2002; Zhang et al., 2004); moreover, Leu-Ile derives from FK506, which exerts neuroprotective action through Hsp70 (Gold et al., 2004). Therefore, the band of ~70 kDa was selected and processed to generate tryptic peptides, which was analyzed by direct nanoflow LC-MS. All of the digested peptide fragments could be assigned to Hsc70 with 100% homology by Mascot Search, and the matching score was 496 (Fig. 2*C*,*D*). To confirm the mass spectrometric-based identification of the Leu-Ile-binding protein, reaction complexes were subjected to SDS-PAGE and immunoblotted with Hsc70 antibody. We detected Hsc70 (open arrow) as well as an Hsc70-Leu-Ile complex (closed arrow), which showed a slight retardation of electrophoretic mobility because of the increased molecular weight compared with that of Hsc70 (Fig. 2*E*). Moreover, Hsc70-Leu-Ile (closed arrow) and Hsc70 (open arrow) were also identified by CBB staining in the reaction complex of Leu-Ile with recombinant Hsc70 (Fig. 2*F*). These results confirm that Hsc70 is a specific binding protein for Leu-Ile.

To study whether FK506 binds to Hsc70, Leu-Ile or FK506 Affigel-10 were incubated with brain homogenate at 4°C overnight. The eluants were subjected to SDS-PAGE and probed with anti-Hsc70 antibody. Interestingly, Hsc70 was detected in the eluants from both Leu-Ile and FK506 Affigel-10, suggesting that Hsc70 may bind to FK506 directly or indirectly (Fig. 2*G*).

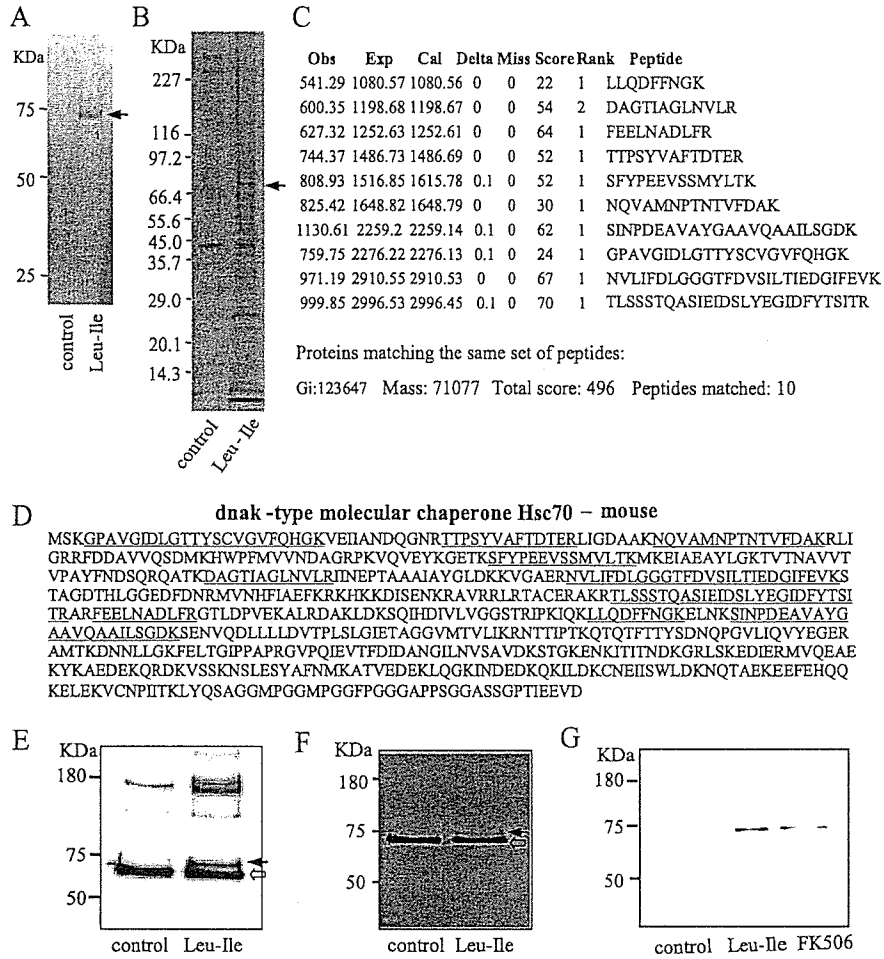

Figure 2. Identification of the specific protein binding to Leu-Ile. ***A***, The reaction complexes of brain homogenate and FITC-Leu-Ile were subjected to gel electrophoresis, followed by fluorescent scanning. FITC-Leu-Ile alone was used as a control. The protein binding with FITC-Leu-Ile is marked by an arrow. ***B***, Brain homogenate was incubated with Leu-Ile Affigel-10 followed by washing and elution. The eluates were separated by electrophoresis, followed by silver staining. The protein band (arrow) was analyzed by mass spectrometry. ***C***, The figure incorporates the observed mass (Obs), expected nominal mass (Exp), and calculated mass (Cal), together with the Miss, Score, Rank from Mascot Search, and Peptide sequence. ***D***, The picture shows the amino acid sequence assigned to each peptide (underlined) and their position in the Hsc70 sequence (NCBI, Gi:123647). ***E***, Brain homogenate was or was not (control) reacted with Leu-Ile, and the reaction complex was subjected to SDS-PAGE followed by immunoblotting with anti-Hsc70 antibody. Leu-Ile-Hsc70 (closed arrow) and Hsc70 (open arrow) are shown. ***F***, Recombinant Hsc70 was or was not (control) reacted with Leu-Ile, and the reaction complexes were subjected to SDS-PAGE followed by CBB staining. Leu-Ile-Hsc70 (closed arrow) and Hsc70 (open arrow) are shown. ***G***, Brain homogenate was incubated with Leu-Ile- or FK506-Affigel, followed by washing and elution. The eluates were separated by electrophoresis and probed with anti-Hsc70 antibody.

Interaction between Leu-Ile and Hsc70

QCM was applied to investigate more directly the interaction between Leu-Ile and Hsc70. The resonance frequency change ($-\delta F$) of QCM responding to Leu-Ile decreased over time, indicating that Hsc70 had a significant affinity for Leu-Ile in a time-dependent manner (Fig. 3*A*). However, Pro-Leu and Ile-Pro had no effect on the resonance frequency change. The resonance frequency was decreased dose-dependently by Hsc70, showing the affinity of Hsc70 for Leu-Ile with K_d equal to 1.83×10^{-8} M (Fig. 3*B*). Leu-Ile had no influence on resonance frequency change when it was incubated with heat-denatured Hsc70 (data not shown). These results indicate the binding specificity of these two molecules and the requirement of the three-dimensional conformations of Hsc70 and Leu-Ile. However, resonance frequency change was not observed when Hsc70 was added to the QCM plate immobilized with FK506, suggesting that FK506 may not bind directly to Hsc70 (Fig. 3*C*).

ATPase domain of Hsc70 is the predicted binding site of Leu-Ile

To get further insights for Leu-Ile-Hsc70 interaction, three-dimensional structural models of ATPase domain, substrate-

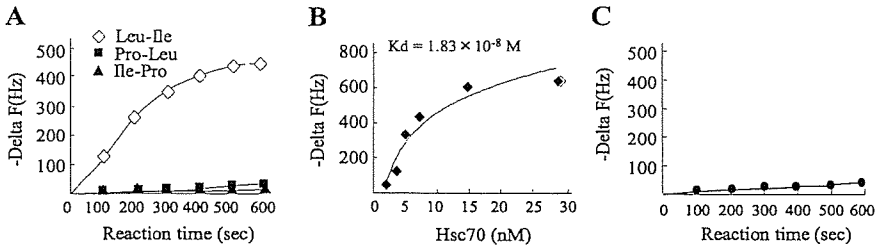

Figure 3. Affinity of Leu-Ile and Hsc70 was assayed by QCM. *A*, Time course of frequency change ($-\delta$ F) of dipeptide-immobilized QCM is shown, responding to the addition of Hsc70 to the aqueous solution. *B*, Binding behavior of Leu-Ile to Hsc70 is dependent on Leu-Ile concentration. *C*, Frequency change of FK506-immobilized QCM was not observed with Hsc70.

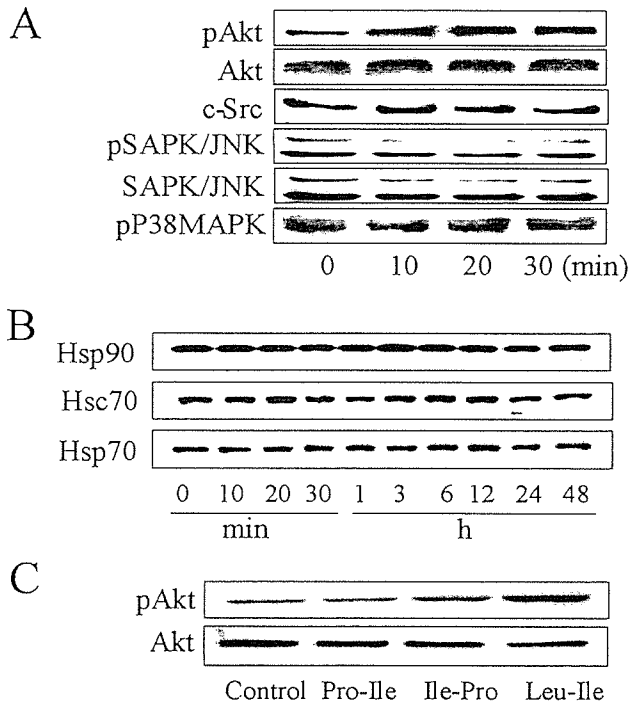

Figure 4. Leu-Ile stimulates Akt phosphorylation. *A*, Neurons were exposed to Leu-Ile (10 μg/ml) for the indicated times. Cell lysates were subjected to SDS-PAGE and probed with various antibodies. The representative immunoblots are shown. *B*, Neurons were exposed to Leu-Ile (10 μg/ml) for the indicated times. Immunoblots were probed with antibodies against Hsp90, Hsp70, and Hsc70. *C*, Neurons were stimulated with Leu-Ile, Pro-Leu, and Ile-Pro (10 μg/ml) for 30 min. Cell lysates were subjected to SDS-PAGE and probed with antibodies against pAkt and Akt.

binding domain, or C-terminal domain of Hsc70 were produced, and the potential interaction of each domain with Leu-Ile was analyzed by MOE software. The ATPase domain showed the strongest interaction potential with Leu-Ile among these three domains. The predicted binding site of Leu-Ile in this domain appears to be a pocket structure, which is near the ADP docking site (supplemental Fig. 1*A*, available at www.jneurosci.org as supplemental material). It has been demonstrated that substrates, binding at this domain, affect the ATP cycle and cause conformational regulation of Hsc70 and its cochaperones (Hernández et al., 2002). The substrate-binding domain showed no stable docking site for Leu-Ile (supplemental Fig. 1*B*, available at www.jneurosci.org as supplemental material).

Leu-Ile stimulates Akt phosphorylation

Because Hsc70/Hsp90 cochaperones modulate the activities of a restricted number of tyrosine and serine/threonine kinases (Nollen and Morimoto, 2002), we first investigated whether c-Src, P38MAPK, SAPK/JNK, and Akt were affected by Leu-Ile. The pAkt level was elevated by Leu-Ile (10 μg/ml) treatment for 20 or 30 min (Fig. 4*A*), whereas no changes in levels of other kinases were observed. In addition, expressions of Hsp90, Hsp70, and Hsc70 were not affected by Leu-Ile treatment for the indicated time points, showing that Leu-Ile is not a heat shock response inducer (Fig. 4*B*). Another two peptides, Pro-Leu and Ile-Pro, could not promote Akt phosphorylation (Fig. 4*C*).

Leu-Ile-induced Akt phosphorylation is mediated by Hsp90

As shown in Figure 5*A*, Akt phosphorylation was stimulated after Leu-Ile treatment for 20 or 30 min [$F_{(5,18)} = 11.30$; $p < 0.01$ and $p < 0.01$ respectively, compared with the control (0 min)]. Because Hsp90 is a modulator for Akt, we thus investigated whether Akt activation by this dipeptide was mediated through Hsp90. The cultures were exposed to an Hsp90 inhibitor GA (10 μM) for 3 h, followed by Leu-Ile stimulation for 30 min. We found that the increase in pAkt level induced by Leu-Ile was obviously abolished by GA pretreatment ($p < 0.01$, compared with Leu-Ile treatment for 30 min). GA did not cause toxicity to neurons in our cultures (data not shown). To evaluate the involvement of PI3-k, an upstream activator for Akt, the cultures were stimulated by Leu-Ile after pretreatment with a PI3-k inhibitor LY294002 (15 μM) for 2 h. Although the pAkt level induced by Leu-Ile was inhibited by LY294002 to some degree, it was still much higher than that of LY294002 alone ($F_{(5,18)} = 11.05$; $p < 0.01$) (Fig. 5*B*), suggesting that Leu-Ile-activated Akt may not be mediated by PI3-k. Furthermore, immunoblotting of immunoprecipitates with anti-Hsp90 antibody was performed using anti-Akt or anti-pAkt antibody. The level of immunoprecipitated pAkt was elevated significantly by Leu-Ile stimulation for 20 or 30 min [$F_{(3,12)} = 7.75$; $p < 0.01$ and $p < 0.01$ respectively, versus control (0 min)] (Fig. 5*C*, top), indicating the enhanced interaction between Hsp90 and pAkt. Although immunoprecipitated Akt did not differ significantly, the increase tendency was obvious (Fig. 5*C*, middle). Direct interaction between Hsc70 and Akt was not observed in our immunoprecipitation assays (data not shown). Together, Leu-Ile is considered to activate Akt in an Hsp90-dependent manner.

CREB is a downstream target of Hsp90/Akt signaling activated by Leu-Ile

CREB was chosen to study intensively because it is a regulatory target of Akt and closely associated with GDNF expression. The amount of pCREB at Ser^{133} was increased after Leu-Ile stimulation for 20 or 30 min (Fig. 6*A*), whereas both Pro-Leu and Ile-Pro could not promote CREB phosphorylation (Fig. 6*B*). Moreover, increased pCREB immunoreactivity and nucleus translocation induced by Leu-Ile were observed in MAP2-positive cells (Fig. 6*C*, middle), which is thought to be an early step for gene transcriptional regulation of CREB. To study the possibility of Leu-Ile acting on glial cells, both GFAP and pCREB were stained, despite that the culture contained few glial cells. We found that enhanced pCREB immunoreactivity and nucleus translocation induced by

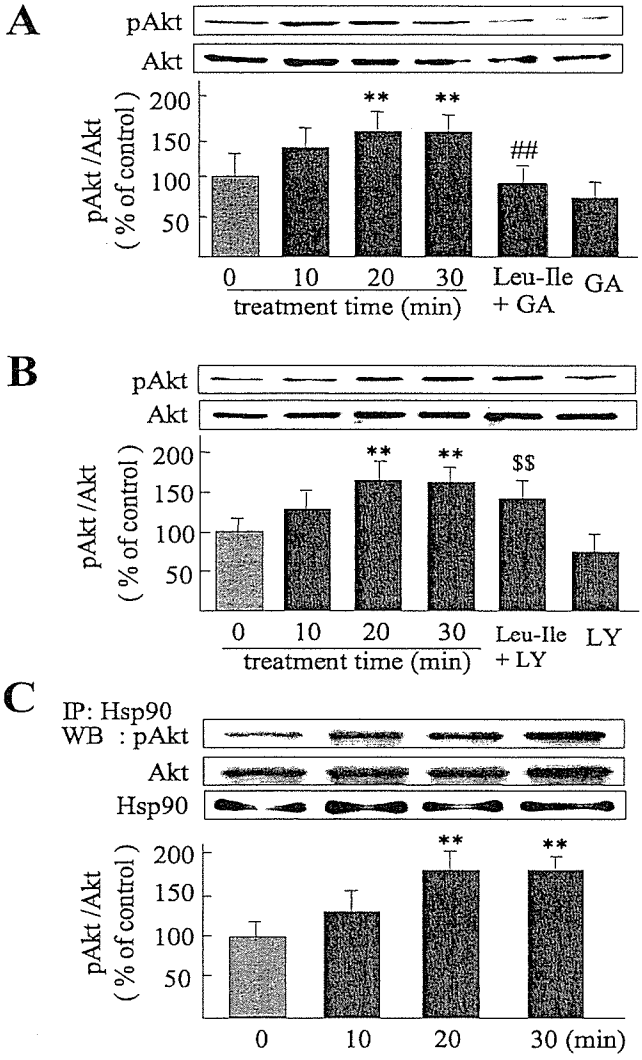

Figure 5. Akt activation induced by Leu-Ile is mediated by Hsp90. ***A***, ***B***, Neurons were stimulated with Leu-Ile (10 μg/ml) alone for 0, 10, 20, and 30 min, or pretreated with GA (10 μM) for 3 h (***A***) or LY294002 (15 μM) for 2 h (***B***), followed by Leu-Ile (10 μg/ml) treatment for 30 min. Cell lysates were immunoblotted with antibodies against pAkt and Akt. Each column represents the mean ± SEM ($n = 4$). Leu-Ile + GA neurons were pretreated with GA followed by Leu-Ile; GA neurons were pretreated with GA alone; Leu-Ile + LY neurons were pretreated with LY294002 followed by Leu-Ile treatment; LY neurons were pretreated with LY294002. $^{**}p < 0.01$ versus control (0 min); $^{\#\#}p < 0.01$ versus Leu-Ile (30 min); $^{\$\$}p < 0.01$ versus LY294002. ***C***, Cultures were exposed to 10 μg/ml of Leu-Ile for the periods indicated. Cell extracts were immunoprecipitated (IP) with anti-Hsp90 antibody or control rabbit IgG, followed by immunoblotting (WB). Densitometric data are presented as the mean ± SEM ($n = 4$). $^{**}p < 0.01$ versus control (0 min).

Leu-Ile were not located in GFAP-positive cells, which showed lower pCREB immunoreactivity (Fig. 6*D*). To assess the involvement of Hsp90/Akt signaling in CREB phosphorylation induced by Leu-Ile, we investigated the change of pCREB after inhibition of this pathway. The cultures were stimulated with Leu-Ile alone for 10, 20, or 30 min, or pretreated with GA (10 μM) for 3 h, followed by Leu-Ile treatment for 30 min. We found that the pCREB level was elevated after Leu-Ile exposure for 20 or 30 min [$F_{(5,18)} = 11.32$; $p < 0.01$ and $p < 0.01$ respectively, compared with control (0 min)], whereas the increase was inhibited by GA pretreatment ($p < 0.01$ versus Leu-Ile for 30 min) (Fig. 6*E*). Double-staining supported these results, showing the loss of pCREB immunoreactivity and nucleus translocation in GA-treated neurons (Fig. 6*C*, bottom). The increase in pCREB induced by Leu-Ile could not be inhibited by LY294002, and showed a higher level compared with LY294002 group ($F_{(5,18)} = 10.36$; $p < 0.01$) (Fig. 6*F*). Because a wide range of neuromodulators can converge on CREB via various cascades in neurons, we examined pERK1/2, PKC, and pCaMKIIα/β. However, no changes of these kinases were observed responding to Leu-Ile (Fig. 6*G*). Collectively, these results show that CREB is a downstream target of Hsp90/Akt signaling activated by Leu-Ile.

Leu-Ile increases GDNF expression in a CREB-dependent manner

After the cultures were exposed to 10 μg/ml Leu-Ile, Pro-Leu, or Ile-Pro for 24 h respectively, the levels of GDNF expression were measured. We found that Leu-Ile, but not Pro-Leu and Ile-Pro, significantly promoted GDNF production (Fig. 7*A*). Moreover, the levels of GDNF mRNA were obviously elevated when neurons were incubated with Leu-Ile (10 μg/ml) for 12 or 18 h, as evidenced by real-time RT-PCR measurement (Fig. 7*B*). These results were well consistent with our previous report (Nitta et al., 2004). To investigate the role of CREB in transcriptional regulation of the GDNF gene induced by Leu-Ile, CREB antisense ODN was used to downregulate CREB expression. CREB expression was inhibited when neurons were transfected with CREB antisense ODN for 24 h, whereas sense ODN showed no effect (Fig. 7*C*). GDNF mRNA levels were measured after Leu-Ile treatment for 18 h in the presence of CREB antisense ODN or sense ODN, and we found that GDNF mRNA induced by Leu-Ile was inhibited significantly by CREB antisense ODN (Fig. 7*D*). Furthermore, cellular GDNF expression was analyzed after Leu-Ile treatment in the presence of CREB antisense ODN. The GDNF level was dramatically elevated to ~188% after neurons were incubated with Leu-Ile for 24 h ($F_{(5,18)} = 25.74$; $p < 0.001$ versus control). However, the induction of GDNF expression by this dipeptide was significantly attenuated by CREB antisense ODN ($p < 0.01$ versus Leu-Ile or Leu-Ile plus CREB sense ODN). CREB antisense ODN did not significantly influence the basal expression of GDNF (Fig. 7*E*). Similarly, immunostaining revealed both stronger GDNF and nuclear pCREB immunoreactivities in Leu-Ile-treated neurons (Fig. 7*F*, middle), whereas such actions were blocked by CREB inhibition resulted from antisense ODN (Fig. 7*F*, right). These observations indicated that GDNF expression was in parallel with CREB phosphorylation. Additionally, pCREB-CRE binding activity was obviously promoted after Leu-Ile treatment for 30 min ($F_{(3,12)} = 51.28$; $p < 0.01$ compared with control) (Fig. 7*G*, left two columns). Competitive experiments showed the specificity of pCREB-CRE binding, because the increased pCREB-CRE binding activity was almost totally blocked when competitive wild-type ODN probe was added ($p < 0.001$ versus mutant ODN treatment), but not the mutant one (Fig. 7*G*, right two columns). Collectively, these results showed that CREB plays a key role in transcriptional regulation of the GDNF gene induced by Leu-Ile.

Discussion

Using the principles of structure-based drug design, we synthesized three dipeptide analogs which resemble the dipeptide-like binding site of FK506 for immunophilin. Among these dipeptides, hydrophobic Leu-Ile was demonstrated to promote GDNF expression. Transport studies revealed the transmembrane mobility of Leu-Ile, although it is not clear which pathway is responsible for this process. Peptide transporter PTH1 is considered to transport oligopeptides, especially dipeptides, into neurons (Ya-

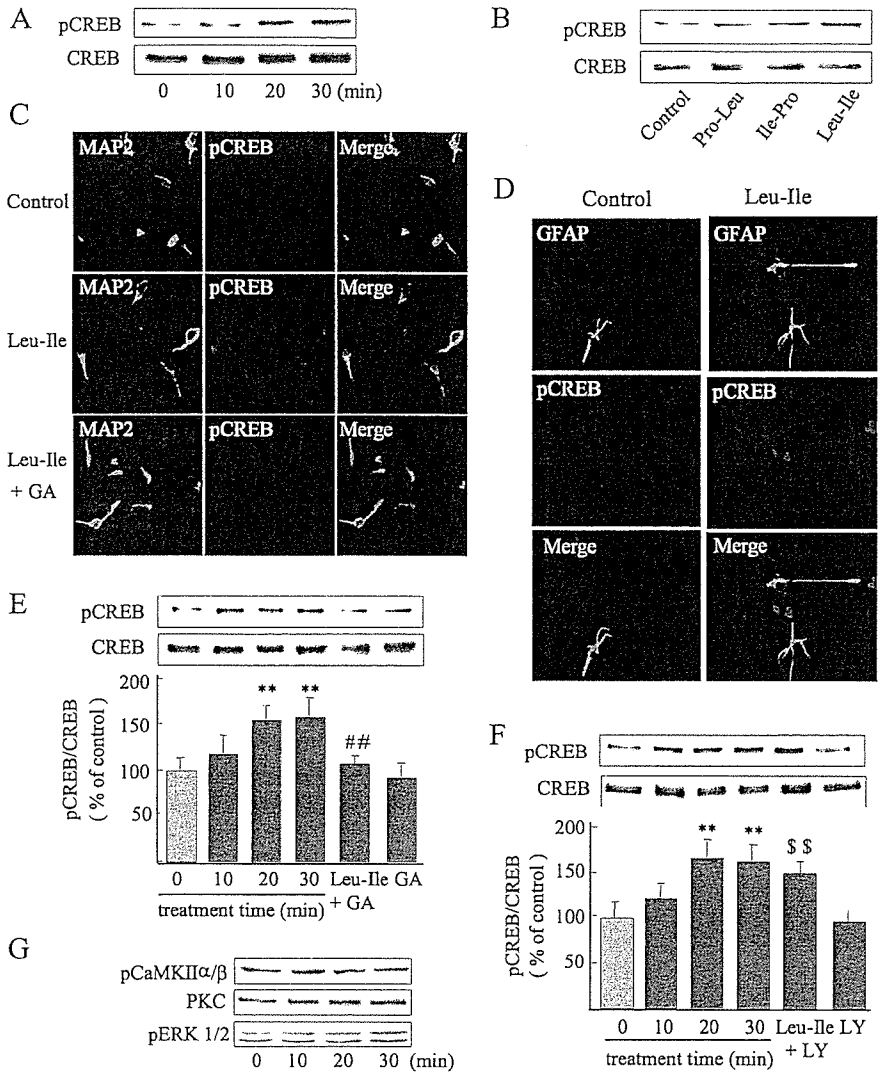

Figure 6. CREB is a downstream target of Hsp90/Akt signaling activated by Leu-Ile. ***A***, Cultured neurons were exposed to 10 μg/ml of Leu-Ile for 0, 10, 20, and 30 min, and pCREB was measured by immunoblotting. ***B***, Western blotting with anti-pCREB antibody reveals CREB activation induced by Leu-Ile but not Pro-Leu and Ile-Pro. ***C***, Visualization of CREB phosphorylation (red) in MAP2-positive neurons (green) induced by Leu-Ile. ***D***, Phosphorylated CREB (red) induced by Leu-Ile is not located in GFAP-positive cells (green). ***E***, ***F***, Neurons were treated with Leu-Ile (10 μg/ml) for 0 (control), 10, 20, and 30 min respectively, or pretreated with GA (10 μM) for 3 h (***E***) or LY294002 (15 μM) for 2 h (***F***), followed by Leu-Ile (10 μg/ml) treatment for 30 min. Each column represents the mean ± SEM ($n = 4$). Leu-Ile + GA neurons were pretreated with GA followed by Leu-Ile; GA neurons were pretreated with GA; Leu-Ile + LY neurons were pretreated with LY294002 followed by Leu-Ile; LY neurons were pretreated with LY294002. $^{**}p < 0.01$ versus control (0 min); $^{\#\#}p < 0.01$ versus Leu-Ile (30 min); $^{\$\$}p < 0.01$ versus LY294002. ***G***, PKC, pERK1/2, and pCaMKIIα/β were measured after Leu-Ile (10 μg/ml) treatment by immunoblotting.

mashita et al.,1997), and Leu-Ile is possibly transported by this transporter.

A series of experiments indicated that Leu-Ile binds specially to Hsc70, a member of the heat shock protein 70 family, which represents an important cellular mechanism in chaperone-mediated neuroprotection (Muchowski, 2002). The binding of Hsc70 to Leu-Ile was time and dose dependent, as suggested by QCM measurement. Moreover, such binding depended on the dimensional structure of both Hsc70 and Leu-Ile, because heat-denatured Hsc70 failed to bind this dipeptide, and another two similar dipeptides, Pro-Leu and Ile-Pro, showed no affinity for Hsc70. These findings indicate that Leu-Ile-Hsc70 interaction may be not a transient association but a specific binding dependent on their dimensional structure. By molecule modeling and docking stimulation, the ATPase domain of Hsc70 rather than the substrate-binding domain is shown to be the predicted binding site for Leu-Ile. It is known that Hsc70 interacts with co-chaperones through the ATPase domain and that binding of exposed stretches of hydrophobic residues in proteins or peptides is regulated by ATP-hydrolysis-induced conformational changes in the ATPase domain (Nollen et al., 2001). Therefore, the interaction between Leu-Ile and Hsc70 may result in conformational and functional regulation of Hsc70.

Hsc70/Hsp90 chaperones are specially considered to be an integrated cochaperone machinery. They often work together as essential components of a process that alters the conformations of a certain number of signaling transducers to states that respond in signal transduction, such as glucocorticoid receptors, Akt, and Src kinases (Rajapandi et al., 2000; Pearl and Prodromou, 2001). Moreover, activities of Hsc70/Hsp90 machinery are affected by a wide range of cofactor proteins that interact directly and specifically with either Hsc70 or Hsp90, and modulation of Hsc70 ATPase may affect the functions of Hsp90 toward its client proteins. We thus proposed that Leu-Ile, after binding to Hsc70, influenced Hsc70/Hsp90 chaperoning function toward client signaling proteins, resulting in mobilization of downstream signaling. To explore this hypothesis, we first studied some tyrosine and serine/threonine kinases, including mitogen-activated protein kinases, Akt, and Src, which are closely associated with Hsp90 and neuron survival (Richter and Buchner, 2001). Akt phosphorylation was elevated apparently by Leu-Ile, whereas other kinases showed no change, implying the functional modulation of Hsc70 by Leu-Ile and involvement of Hsc70/Hsp90 co-chaperone in the regulation of Akt phosphorylation. Thulasiraman et al. (2002) reported a similar finding that a small hydrophobic peptide, binding to the ATPase domain of Hsc70, affects ATPase activity and Hsp90/Hsc70-dependent transformation of eukaryotic initiation factor 2α kinase into an active form.

Heat shock response has been implicated in mediating the neuroprotective effect of FK506 (Klettner and Herdegen, 2003; Gold et al., 2004) and in activating Akt by conformational regulation of this molecule (Konishi et al., 1999; Matsuzaki et al., 2004). However, Leu-Ile did not affect the expression of Hsc70, Hsp70, or Hsp90, indicating that it unlikely exerts neuroprotective action by a mechanism of heat shock response. Given the possibility that the binding of FK506 to Hsp90/steroid receptor complexes might dissociate Hsp90 from heat shock factor, thus inducing heat shock response (Gold et al., 1999, 2004; Klettner and Herdegen, 2003), Leu-Ile unlikely affects the association between Hsp90 and steroid receptor, which may underlie its incapability in inducing heat shock response.

GA is known to bind the ATP-binding pocket of Hsp90 and to inhibit ATP binding and hydrolysis, thereby disrupting its function (Basso et al., 2002). GA significantly blocked the increased pAkt levels induced by Leu-Ile, whereas PI3-k inhibitor LY294002 failed. On the basis of these findings, Leu-Ile is considered to activate Akt through Hsp90. It is clear that Akt interacts with Hsp90 via its catalytic domain and that Hsp90 promotes Akt activity by reducing PP2A-mediated pAkt dephosphorylation at the threonine 308 residue (Sato et al., 2000). Therefore, Leu-Ile, after binding to Hsc70, may facilitate Hsp90-Akt interaction through conformational regulation, resulting in an increase in pAkt through protecting it from dephosphorylation. Immunoprecipitation assays demonstrated such hypothesis because it revealed a significant increase in pAkt-Hsp90 interaction. We also observed an elevation in total Akt immunoprecipitated by Hsp90 despite that the difference was not significant. Considering that GA causes the ubiquitin-mediated degradation of client Akt (Prodromou et al., 1997), Leu-Ile may inhibit proteasomal degradation of Akt mediated by Hsc70/Hsp90, resulting, accordingly, in pAkt elevation. This notion is supported by previous studies, which show that CAIR-1, after binding to the Hsc70 ATPase domain, increases Akt phosphorylation by inhibiting its shift from Hsp90 to Hsc70, where Akt is ubiquitinated and degraded (Doong et al., 2003). Our data cannot distinguish between these two mechanisms. Anyway, Hsc70, after binding to Leu-Ile, appears to be crucial for the transmitting of neurotrophic signals of this dipeptide, which brings about Hsp90/Akt signaling. Nakagomi et al. (2003) reported that Hsp27 promotes survival in PC12 cells and ganglion neurons by promoting Akt activity, which is independent of upstream activators. A chaperone-like protein, β-synuclein, exerts a neuroprotective effect by directly stabilizing Akt activity rather than by acting on PI3-k (Hashimoto et al., 2004). Therefore, these findings, together with ours, further support a notion that chaperones like Hsp90 may participate in neuroprotection by conformational or chaperoning modulation of Akt rather than by acting on upstream effectors of the pathways. Additionally, Akt activation is required for increased expression of astroglial GDNF induced by melatonin (Lee et al., 2006).

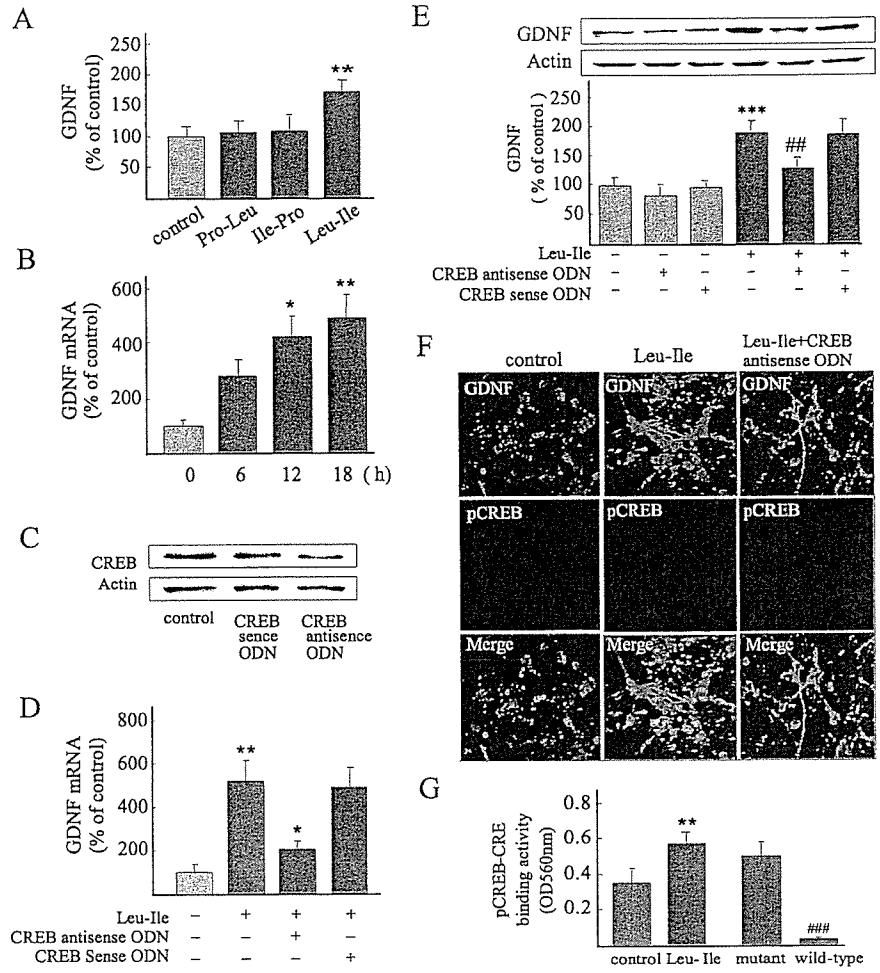

Figure 7. Leu-Ile increases GDNF expression in a CREB-dependent manner. ***A***, Leu-Ile significantly increased GDNF expression, whereas Pro-Leu and Ile-Pro showed no GDNF-inducing activities. $^{**}p < 0.01$ versus control ($n = 4$). ***B***, GDNF mRNA levels induced by Leu-Ile for various periods were studied by real-time RT-PCR. $^{*}p < 0.05$ and $^{**}p < 0.01$ versus control (0 h). ***C***, CREB expression was blocked by CREB antisense ODN, as revealed by Western blotting. ***D***, Neurons were incubated with Leu-Ile (10 μg/ml) for 24 h in the presence of CREB antisense ODN or sense ODN. Data are expressed as a percentage of the control (mean ± SEM; $n = 4$). $^{**}p < 0.01$ versus control; $^{*}p < 0.05$ versus Leu-Ile or Leu-Ile plus CREB sense ODN. ***E***, Neurons were incubated with Leu-Ile (10 μg/ml) for 24 h in the presence of CREB antisense ODN or sense ODN. Data are expressed as a percentage of control (mean ± SEM; $n = 4$). $^{***}p < 0.001$ versus control; $^{\#\#}p < 0.01$ versus Leu-Ile or Leu-Ile plus CREB sense ODN. ***F***, Neurons were labeled with anti-GDNF (green) and anti-pCREB antibodies (red). ***G***, CRE-pCREB binding activities were quantified after Leu-Ile treatment for 30 min. $^{**}p < 0.01$ versus control; $^{\#\#\#}p < 0.001$ verse mutant ODN ($n = 4$).

GA blocked CREB activation induced by Leu-Ile, indicating that CREB activation proceeds via Hsp90/Akt signaling. These findings are supported by previous studies that show that modulation of Akt based on Hsc70/Hsp90 cochaperones results in the maintenance of downstream CREB activation (Doong et al., 2003). Although CRE exists in the promoter sequence of the GDNF gene, there is no direct evidence showing the role of CREB in GDNF transcriptional regulation. Moreover, Akt promotes phosphorylation of CREB, stimulates recruitment of CREB to promoters, and activates gene expression (Pugazhenthi et al., 2000; Leinninger et al., 2004). We thus intensively investigated the role of Leu-Ile-activated pCREB in GDNF expression. We found that Leu-Ile-induced GDNF mRNA production and protein expression were attenuated when CREB was inhibited. Furthermore, CREB activation was accompanied by an increased capacity to activate transcription of target genes, because pCREB-CRE-binding activity was promoted. These results demonstrated that CREB-dependent transcriptional regulation is responsible for the GDNF-inducing properties of Leu-Ile. Although GDNF expression likely involves combinatorial interactions with multiple transcription factors including CREB, nuclear factor κB (NF-κB), and AP-2 (Woodbury et al., 1998), Leu-Ile-induced CREB activation is sufficient for inducing GDNF expression, indicating that CREB functions as an important transcriptional factor for the GDNF gene. Similarly, FK960 induces GDNF expression in CREB-dependent mechanisms (Koyama et al., 2004). The extent to which a transcription factor is required for GDNF

transcriptional regulation is likely to depend on the character, strength, or duration of extracellular stimuli. For example, NF-κB seems to play a role in GNDF induction in response to cytokines (Tanaka et al., 2000), whereas CREB likely participates in GNDF induction by growth factors like basic fibroblast growth factor (Lenhard et al., 2002). The defined Hsp90/Akt/CREB pathway may provide a novel significant signaling that regulates GDNF expression.

Several cascades have been implicated in underlying neurotrophic activity of FK506. For example, FK506 potentiates NGF-induced neurite outgrowth via the Ras/Raf/MAPK pathway and involves PI3-k signaling (Price et al., 2003, 2005). Gold et al. (1999) reported that GA blocked neurotrophic action of FK506, suggesting FK506 interaction with Hsp90 via binding to FKBP52 is important for its neuroregenerative properties. However, FKBP-12 is not necessary for its neurotrophic effects (Gold et al., 1999, 2005). As suggested from QCM findings, FK506 may not interact with Hsc70 directly. Although the role of Hsc70 in mediating neuroprotective action of FK506 is unclear at present, it is tempting to speculate that FK506 might regulate the chaperoning function of Hsp90/Hsc70 through FKBP and, thus, modulate certain signaling kinases. It remains to be investigated intensively.

GDNF is a promising therapeutic agent for the treatment of neurodegenerative diseases. However, the delivery of GDNF to the CNS provides an interesting challenge, because GDNF is unable to cross the blood–brain barrier (Kirik et al., 2004), and use of low-molecular-weight drugs is an interesting alternative. FK506 exerts neuroprotective action, which is thought to depend on its GDNF-promoting effect (Tanaka et al., 2003). However, it cannot be used in therapy for neurological disorders because of its immunosuppressive effects. Leu-Ile, a small hydrophobic molecule, can penetrate neurons and promote GDNF expression, although it shows no immunosuppressive activity. Thus, it may represent a novel lead compound for treatment of dopaminergic neuron or motoneuron diseases such as Parkinson disease.

In conclusion, Leu-Ile targets the Hsc70/Hsp90 cochaperone and, thus, triggers Akt/CREB signaling, resulting in upregulation of GDNF expression. This defined cascade may provide a deep insight into the cellular mechanism of GDNF expression regulation.

References

Airaksinen MS, Saarma M (2002) The GDNF family: signalling, biological functions and therapeutic value. Nat Rev Neurosci 3:383–394.

Baecker PA, Lee WH, Verity AN, Eglen RM, Johnson RM (1999) Characterization of a promoter for the human glial cell line-derived neurotrophic factor gene. Mol Brain Res 69:209–222.

Basso AD, Solit DB, Chiosis G, Giri B, Tsichlis P, Rosen N (2002) Akt forms an intracellular complex with heat shock protein 90 (Hsp90) and Cdc37 and is destabilized by inhibitors of Hsp90 function. J Biol Chem 277:39858–39866.

Brami-Cherrier K, Valjent E, Garcia M, Pagès C, Hipskind RA, Caboche J (2002) Dopamine induces a PI3-kinase-independent activation of Akt in striatal neurons: a new route to cAMP response element-binding protein phosphorylation. J Neurosci 22:8911–8921.

Brunet A, Datta SR, Greenberg ME (2001) Transcription-dependent and -independent control of neuronal survival by the PI3K-Akt signaling pathway. Curr Opin Neurobiol 11:297–305.

Castro LM, Gallant M, Niles LP (2005) Novel targets for valproic acid: up-regulation of melatonin receptors and neurotrophic factors in C6 glioma cells. J Neurochem 95:1227–1236.

Chou CC, Forouhar F, Yeh YH, Shr HL, Wang C, Hsiao CD (2003) Crystal structure of the C-terminal 10-kDa subdomain of Hsc70. J Biol Chem 278:30311–30316.

Doong H, Rizzo K, Fang S, Kulpa V, Weissman AM, Kohn EC (2003) CAIR-1/BAG-3 abrogates heat shock protein-70 chaperone complex-mediated protein degradation. J Biol Chem 278:28490–28500.

Du K, Montminy M (1998) CREB is a regulatory target for the protein kinase Akt/PKB. J Biol Chem 273:2377–32379.

Flaherty KM, DeLuca-Flaherty C, McKay DB (1990) Three-dimensional structure of the ATPase fragment of a 70K heat-shock cognate protein. Nature 346:623–628.

Gold BG, Densmore V, Shou W, Matzuk MM, Gordon HS (1999) Immunophilin FK506-binding protein 52 (not FK506-binding protein 12) mediates the neurotrophic action of FK506. J Pharmacol Exp Ther 289:1202–1210.

Gold BG, Voda J, Yu X, Gordon H (2004) The immunosuppressant FK506 elicits a neuronal heat shock response and protects against acrylamide neuropathy. Exp Neurol 187:160–170.

Gold BG, Armistead DM, Wang MS (2005) Non-FK506-binding protein-12 neuroimmunophilin ligands increase neurite elongation and accelerate nerve regeneration. J Neurosci Res 80:56–65.

Hashimoto M, Bar-On P, Ho G, Takenouchi T, Rockenstein E, Crews L, Masliah E (2004) β-Synuclein regulates Akt activity in neuronal cells. A possible mechanism for neuroprotection in Parkinson's disease. J Biol Chem 279:23622–23629.

Hernández MP, Sullivan WP, Toft DO (2002) The assembly and intermolecular properties of the hsp70-Hop-hsp90 molecular chaperone complex. J Biol Chem 277:38294–38304.

Johnson JR, Chu AK, Sato-Bigbee C (2000) Possible role of CREB in the stimulation of oligodendrocyte precursor cell proliferation by neurotrophin-3. J Neurochem 74:1409–1417.

Kirik D, Georgievska B, Bjorklund A (2004) Localized striatal delivery of GDNF as a treatment for Parkinson disease. Nat Neurosci 7:105–110.

Klettner A, Herdegen T (2003) The immunophilin-ligands FK506 and V-10,367 mediate neuroprotection by the heat shock response. Br J Pharmacol 138:1004–1012.

Konishi H, Fujiyoshi T, Fukui Y, Matsuzaki H, Yamamoto T, Ono Y, Andjelkovic M, Hemmings BA, Kikkawa U (1999) Activation of protein kinase B induced by H_2O_2 and heat shock through distinct mechanisms dependent and independent of phosphatidylinositol 3-kinase. J Biochem 126:1136–1143.

Koyama Y, Egawa H, Osakada M, Baba A, Matsuda T (2004) Increase by FK960, a novel cognitive enhancer, in glial cell line-derived neurotrophic factor production in cultured rat astrocytes. Biochem Pharmacol 68:275–282.

Lee SH, Chun W, Kong PJ, Han JA, Cho BP, Kwon OY, Lee HJ, Kim SS (2006) Sustained activation of Akt by melatonin contributes to the protection against kainic acid-induced neuronal death in hippocampus. J Pineal Res 40:79–85.

Lee SJ, Campomanes CR, Sikat PT, Greenfield AT, Allen PB, McEwen BS (2004) Estrogen induces phosphorylation of cyclic AMP response element binding (pCREB) in primary hippocampal cells in a time-dependent manner. Neuroscience 124:549–560.

Leinninger GM, Backus C, Uhler MD, Lentz SI, Feldman EL (2004) Phosphatidylinositol 3-kinase and Akt effectors mediate insulin-like growth factor-I neuroprotection in dorsal root ganglia neurons. FASEB J 18:1544–1556.

Lenhard T, Schober A, Suter-Crazzolara C, Unsicker K (2002) Fibroblast growth factor-2 requires glial-cell-line-derived neurotrophic factor for exerting its neuroprotective actions on glutamate-lesioned hippocampal neurons. Mol Cell Neurosci 20:181–197.

Matsuzaki H, Yamamoto T, Kikkawa U (2004) Distinct activation mechanisms of protein kinase B by growth-factor stimulation and heat-shock treatment. Biochemistry 43:4284–4293.

Matsushita N, Fujita Y, Tanaka M, Nagatsu T, Kiuch T (1997) Cloning and structural organization of the gene encoding the mouse glial cell line-derived neurotrophic factor, GDNF. Gene 203:149–157.

McLaughlin SH, Smith HW, Jackson SE (2002) Stimulation of the weak ATPase activity of human Hsp90 by a client protein. J Mol Biol 315:787–798.

Morshauser RC, Hu W, Wang H, Pang Y, Flynn GC, Zuiderweg ER (1999) High-resolution solution structure of the 18 kDa substrate-binding domain of the mammalian chaperone protein Hsc70. J Mol Biol 289:1387–1403.

Motomiya Y, Ando Y, Haraoka K, Sun X, Iwamoto H, Uchimura T, Maruyama I

(2003) Circulating level of α2-macroglobulin-β2-microglobulin complex in hemodialysis patients. Kidney Int 64:2244–2252.

Muchowski PJ (2002) Protein misfolding, amyloid formation, and neurodegeneration: a critical role for molecular chaperones? Neuron 35:9–12.

Nakagomi S, Suzuki Y, Namikawa K, Kiryu-Seo S, Kiyama H (2003) Expression of the activating transcription factor 3 prevents c-Jun N-terminal kinase-induced neuronal death by promoting heat shock protein 27 expression and Akt activation. J Neurosci 23:5187–5196.

Nitta A, Nishioka H, Fukumitsu H, Furukawa Y, Sugiura H, Shen L, Furukawa S (2004) Hydrophobic dipeptide Leu-Ile protects against neuronal death by inducing brain-derived neurotrophic factor and glial cell line-derived neurotrophic factor synthesis. J Neurosci Res 78:250–258.

Nollen EA, Morimoto RI (2002) Chaperoning signaling pathways: molecular chaperones as stress-sensing "heat shock" proteins. J Cell Sci 115:2809–2816.

Nollen EA, Kabakov AE, Brunsting JF, Kanon B, Hohfeld J, Kampinga HH (2001) Modulation of *in vivo* HSP70 chaperone activity by Hip and Bag-1. J Biol Chem 276:4677–4682.

Pearl LH, Prodromou C (2001) Structure, function and mechanism of the Hsp90 molecular chaperone. Adv Protein Chem 59:157–186.

Pratt WB, Toft DO (2003) Regulation of signaling protein function and trafficking by the hsp90/hsp70-based chaperone machinery. Exp Biol Med 228:111–133.

Price RD, Yamaji T, Matsuoka N (2003) FK506 potentiates NGF-induced neurite outgrowth via the Ras/Raf/MAP kinase pathway. Br J Pharmacol 140:825–829.

Price RD, Yamaji T, Yamamoto H, Higashi Y, Hanaoka K, Yamazaki S, Ishiye M, Aramori I, Matsuoka N, Mutoh S, Yanagihara T, Gold BG (2005) FK1706, a novel non-immunosuppressive immunophilin: neurotrophic activity and mechanism of action. Eur J Pharmacol 509:11–19.

Prodromou C, Roe SM, O'Brien R, Ladbury JE, Piper PW, Pearl LH (1997) Identification and structural characterization of the ATP/ADP-binding site in the Hsp90 molecular chaperone. Cell 90:65–75.

Pugazhenthi S, Nesterova A, Sable C, Heidenreich KA, Boxer LM, Heasley LE, Reusch JE (2000) Akt/protein kinase B up-regulates Bcl-2 expression through cAMP-response element-binding protein. J Biol Chem 275:10761–10766.

Rajapandi T, Greene LE, Eisenberg E (2000) The molecular chaperones Hsp90 and Hsc70 are both necessary and sufficient to activate hormone binding by glucocorticoid receptor. J Biol Chem 275:22597–22604.

Richter K, Buchner J (2001) Hsp90: chaperoning signal transduction. J Cell Physiol 188:281–290.

Roberson ED, English JD, Adams JP, Selcher JC, Kondratick C, Sweatt JD (1999) The mitogen-activated protein kinase cascade couples PKA and PKC to cAMP response element binding protein phosphorylation in area CA1 of hippocampus. J Neurosci 19:4337–4348.

Rubio E, Valenciano AI, Segundo C, Sanchez N, de Pablo F, de la Rosa EJ (2002) Programmed cell death in the neurulating embryo is prevented by the chaperone heat shock cognate 70. Eur J Neurosci 15:1646–1654.

Saini HS, Gorse KM, Boxer LM, Sato-Bigbee C (2004) Neurotrophin-3 and a CREB-mediated signaling pathway regulate Bcl-2 expression in oligodendrocyte progenitor cells. J Neurochem 89:951–961.

Sato S, Fujita N, Tsuruo T (2000) Modulation of Akt kinase activity by binding to Hsp90. Proc Natl Acad Sci USA 97:10832–10837.

Schinelli S, Zanassi P, Paolillo M, Wang H, Feliciello A, Gallo V (2001) Stimulation of endothelin B receptors in astrocytes induces cAMP response element-binding protein phosphorylation and c-fos expression via multiple mitogen-activated protein kinase signaling pathways. J Neurosci 21:8842–8853.

Tanaka K, Fujita N, Ogawa N (2003) Immunosuppressive (FK506) and non-immunosuppressive (GPI1046) immunophilin ligands activate neurotrophic factors in the mouse brain. Brain Res 970:250–253.

Tanaka M, Ito S, Kiuchi K (2000) Novel alternative promoters of mouse glial cell line-derived neurotrophic factor gene. Biochim Biophys Acta 1494:63–74.

Thulasiraman V, Yun BG, Uma S, Gu Y, Scroggins BT, Matts RL (2002) Differential inhibition of Hsc70 activities by two Hsc70-binding peptides. Biochemistry 41:3742–3753.

Verity AN, Wyatt TL, Lee W, Hajos B, Baecker PA, Eglen RM, Johnson RM (1999) Differential regulation of glial cell line-derived neurotrophic factor (GDNF) expression in human neuroblastoma and glioblastoma cell lines. J Neurosci Res 55:187–197.

Woodbury D, Schaar DG, Ramakrishnan L, Black IB (1998) Novel structure of the human GDNF gene. Brain Res 803:95–104.

Xu W, Yuan X, Jung YJ, Yang Y, Basso A, Rosen N, Chung EJ, Trepel J, Neckers L (2003) The heat shock protein 90 inhibitor geldanamycin and the ErbB inhibitor ZD1839 promote rapid PP1 phosphatase-dependent inactivation of AKT in ErbB2 overexpressing breast cancer cells. Cancer Res 63:7777–7784.

Yamashita T, Shimada S, Guo W, Sato K, Kohmura E, Hayakawa T, Takagi T, Tohyama M (1997) Cloning and functional expression of a brain peptide/histidine transporter. J Biol Chem 272:10205–10211.

Yano S, Tokumitsu H, Soderling TR (1998) Calcium promotes cell survival through CaM-K kinase activation of the protein-kinase-B pathway. Nature 396:584–587.

Young D, Lawlor PA, Leone P, Dragunow M, During MJ (1999) Environmental enrichment inhibits spontaneous apoptosis, prevents seizures and is neuroprotective. Nat Med 5:448–453.

Yun BG, Matts RL (2005) Hsp90 functions to balance the phosphorylation state of Akt during C2C12 myoblast differentiation. Cell Signal 17:1477–1485.

Zhang Y, Champagne N, Beitel LK, Goodyer CG, Trifiro M, LeBlanc A (2004) Estrogen and androgen protection of human neurons against intracellular amyloid beta1–42 toxicity through heat shock protein 70. J Neurosci 24:5315–5321.

Available online at www.sciencedirect.com
SCIENCE DIRECT®
Behavioural Brain Research 168 (2006) 137–143
BEHAVIOURAL BRAIN RESEARCH
www.elsevier.com/locate/bbr

Research report

Relapse of methamphetamine-seeking behavior in C57BL/6J mice demonstrated by a reinstatement procedure involving intravenous self-administration

Yijin Yan [a], Atsumi Nitta [a], Hiroyuki Mizoguchi [a], Kiyofumi Yamada [b], Toshitaka Nabeshima [a,*]

[a] *Department of Neuropsychopharmacology & Hospital Pharmacy, Nagoya University Graduate School of Medicine, Showa-ku, Nagoya 466-8560, Japan*
[b] *Laboratory of Neuropsychoparmacology, Graduate School of Natural Science & Technology, Kanazawa University, Kanazawa 920-1192, Japan*

Received 29 August 2005; received in revised form 31 October 2005; accepted 7 November 2005

Abstract

There is an urgent need to develop a reliable mouse model of relapse to address the genetic factors involved in susceptibility to relapse of drug-seeking behavior by using mutant mice. This paper presents a feasible way to reinstate extinguished methamphetamine (METH)-seeking behavior. Male C57BL/6J mice acquired stable nose-poking responses for taking METH after approximately 10 daily 3-h sessions of METH (0.1 mg/kg/infusion) self-administration under a fixed ratio 1 or 2 (FR1/2) schedule. During the self-administration, cue- and hole-lamps indicated the availability of METH and were inactivated simultaneously with each infusion for 5 s. The mice were exposed to extinction training in the absence of METH-paired stimuli (cue- and hole-lamps) and METH infusion, until they met the extinction criterion (less than 25 active responses or 30% of active responses in the stable self-administration phase on 2 consecutive days). METH-paired stimuli (cue- and hole-lamps) during METH self-administration reliably triggered a relapse of METH-seeking behavior in the absence of METH infusion. A combination of non-contingent intravenous (i.v.) priming and self-injected METH also increased the reinstatement of METH-seeking behavior in the absence of METH-paired stimuli (cue- and hole-lamps) and without METH infusion posterior to the self-injection. These results suggest that the mouse model of relapse in our study might provide a new stage for the exploration of genetic factors involved in relapse of drug dependence and of the underlying mechanisms of drugs of abuse.

Keywords: Mouse model of relapse; Methamphetamine; C57BL/6J mice; Extinction; Cue-induced reinstatement; Drug-primed reinstatement; Intravenous self-administration

1. Introduction

A major clinical problem in treating drug abusers or addicts is relapse of drug dependence even after long-term abstinence. To address this issue, an experimental reinstatement procedure has been established in monkeys and rats [37], which reliably represents relapse of drug-seeking behavior in addicts. This is based on findings of similarities in the development of drug dependence between humans and animals, including compulsive drug taking [9,13,24,44,45], cue-induced relapse [14,15,20,30,38], drug-primed relapse [21,26,39] and stress-triggered relapse [38,39] of drug-seeking behavior. In the typical reinstatement paradigm, the ability of acute exposure to drugs or non-drug conditioned cues to reinstate operant conditioning responses is determined following drug self-administration and subsequent extinction of the drug-reinforced behavior [7,37]. Using this paradigm, potential anatomical neuronal substrates and transmitter systems have been identified [18,19,36,39,46], and clinical data support these findings [3,22,23,25,27].

Clinical therapeutic candidates have also been tested using the reinstatement procedure in experimental animals [37,42]. However, no direct evidence has been obtained of genetic factors contributing to susceptibility to relapse although there is evidence of considerable individual variability in the propensity for relapse to drug seeking and taking in human addicts or animals [2,10,12,13,17,42,45]. Since most genetically modified model animal strains are inbred mice, there is an impetus to develop self-administration and reinstatement procedures for

* Corresponding author. Tel.: +81 52 744 2674; fax: +81 52 744 2682.
E-mail address: tnabeshi@med.nagoya-u.ac.jp (T. Nabeshima).

0166-4328/$ – see front matter © 2005 Elsevier B.V. All rights reserved.
doi:10.1016/j.bbr.2005.11.030

mice [6,12,20,26,31,32,37,42]. In the last decade, mouse models of i.v. self-administration have been well developed and used to identify several specific genes involved in the acquisition and maintenance of drug dependence, including serotonin 1B receptor [35], acetylcholine receptor containing the beta2 [32], dopamine transporter [34], mu-opioid receptor [33], cannabinoid receptor 1 [11,40], metabotropic glutamate receptor 5 [8], dopamine D2 receptor [5,10,16], Kir3 potassium channel subunit, Homer 2 [28], Homer 2 [41], activator of G protein signaling 3 [4], etc. In contrast, a model of relapse has only just been established in 129 × 1/SvJ and C57BL/6 mice, respectively, by two groups of researchers [20,26]. Both strains exhibited a conditioned stimulus-induced, but not intraperitoneal (i.p.) cocaine-primed, reinstatement of extinguished cocaine-seeking behavior, although 129 × 1/SvJ mice demonstrated a modest i.v. cocaine-primed reinstatement. However, it seems to be difficult to extend the reinstatement procedures presented in those two reports to transgenic mice since no further study has been published to date. Thus it largely remains to be determined which genes are specifically involved in the propensity for relapse.

Over the past several years, abuse of METH has spread worldwide, resulting in serious health and social issues [2,8,29,43]. Similar to other drugs of abuse, a major clinical concern in the treatment of METH addiction is relapse even after long-term abstinence [2,9,43]. However, no research has been conducted to develop reliable procedures to reinstate METH-seeking behavior in mice. In the present study, a newly developed reinstatement procedure was used to characterize the cue-induced and METH-primed reinstatement of extinguished METH-seeking behavior in C57BL/6J mice.

2. Materials and methods

2.1. Subjects and drugs

Male C57BL/6J mice (8 weeks old; SLC, Japan) weighing 20–25 g were used in this study. All mice were kept in a regulated environment (23 ± 0.5 °C; 50 ± 0.5% humidity) with a 12-h reverse light/dark cycle (lights on between 9:00 a.m. and 9:00 p.m.). Water and food were available ad libitum throughout the experiment unless otherwise noted. All experiments were performed in accordance with Guidelines for Animal Experiments of the Nagoya University School of Medicine, the Guiding Principles for the Care and Use of Laboratory Animals approved by the Japanese Pharmacological Society, and the National Institutes of Health Guide for the Care and Use of Laboratory Animals. METH hydrochloride (Dainippon Pharmaceutical, Osaka, Japan) was dissolved in sterile saline and self-administered at a dose of 0.1 mg/kg/infusion over 5 s (infusion volume, 2.1 μl). The unit dose for METH self-administration is based on previous reports [1,6] and our pilot observations.

2.2. Apparatus for nose-poking task and self-administration

Nose-poking task and the subsequent self-administration were conducted in standard mouse operant conditioning chambers (ENV-307A, Med Associates, Georgia, Vermont, USA) located within ventilated sound attenuation cubicles.

For nose-poking task, the chamber was equipped with two nose-poke sensors (ENV-313M, Med Associates) in two holes, two cue-lamps in and above each hole, and a food pellet dispenser (ENV-203-20, Med Associates) connected with a rectangular opening (2.25 cm × 2.25 cm) between the two holes. The bottom of the opening was 5 mm above the chamber floor and was equidistant from the holes. A house light was located at the top of the chamber opposite the holes. During the training period, nose-poking responses in the active hole resulted in the delivery of a pellet to the opening by the dispenser (ENV302M, Med Associates). Nose-poking responses in the inactive hole had no programmed consequences but were recorded by the software MED-PC for Windows (Med Associates).

For self-administration, the operant conditioning chambers were equipped with nose-poke sensors (ENV-313M, Med Associates) in two holes located on one side of the chamber 1.0 cm above the floor, cue- and hole-lamps located, respectively, above and in each hole, and a red house light located on the top of the chamber opposite the holes. Nose-poking responses in one hole (the active hole) activated an infusion pump (PHM-100, Med Associates) and led to the inactivation of METH-associated cues (cue- and hole-lamps). Nose-poking responses in the other hole (the inactive hole) had no programmed consequences but were recorded by the software MED-PC for Windows. The components of the infusion line were connected to each other from the injector to the exit port of the mouse's catheter by joint FEP tubing (inner diameter, 0.25 mm; outer diameter, 0.55 mm; Eicom Co., Ltd., Japan), which was encased in steel spring leashes (Instech, Plymouth Meeting, PA, USA). Swivels were suspended above the operant conditioning chamber. One pump/syringe set was used for each self-administration chamber located inside of the cubicle.

2.3. Nose-poking training under food-deprived conditions

Nose-poking training was conducted in the standard operant chamber mentioned above. Mice were deprived of food for at least 12 h and then trained to make nose-poking responses to food pellet (dustless precision pellets 20 mg, A Holton Industries Co., Frenchtown, NJ, USA) reinforcement under a fixed ratio 1 (FR1) schedule for 2–8 h. After the nose-poking response training, mice were returned to home cages for at least 24 h before surgery.

2.4. Catheter implantation

At least 24 h following the nose-poking training, mice were anesthetized with pentobarbital sodium (50 mg/kg, i.p.). Indwelling catheters were constructed using a micro-silicone tube (inner diameter, 0.50 mm; outer diameter, 0.7 mm; IMG, Imamura Co., Ltd., Japan) and a polyethylene tube (inner diameter, 0.50 mm; outer diameter, 0.8 mm). Incisions were made on the skin of the head and ventral neck, and the right jugular vein was externalized. The end of the catheter was inserted into the jugular vein via a small incision and was secured to the vein and surrounding tissue with silk sutures. The exit port of the catheter passed subcutaneously to the top of the skull where it was attached to a modified 24-gauge cannula, which was secured to the mouse's skull with quick self-curing acrylic resin (Shofu Inc., Japan). To extend their patency, the catheters were flushed immediately after surgery, and in the morning and evening of the days that followed, with 0.03 ml of an antibiotic solution of cefmetazole sodium (20.0 mg/ml; Sankyo Co., Ltd., Japan) dissolved in heparinized saline (70 U/ml; Leo Pharmaceutical Products, Ltd., Japan). Patency was usually confirmed by taking blood back from the catheter. The intravenous injection of 0.15 ml of pentobarbital sodium solution was also used for such a purpose in a few cases (e.g. responses of mice were much different from the previous session in the same phase).

2.5. Saline or METH self-administration

After recovery from surgery, saline or METH self-administration was conducted for 10 consecutive daily 3-h sessions during the light cycle under an FR1 (day 1–4) to FR2 (day 5–10) schedule of saline or METH reinforcement. METH was self-administered at a dose of 0.1 mg/kg/infusion over 5 s (infusion volume, 2.1 μl) for the METH self-administration group of mice ($n = 50$). Saline was self-administered at 2.1 μl/infusion over 5 s for the saline self-administration group of mice ($n = 5$). The house light was illuminated throughout the session. Nose-poking responses in the active hole resulted in a 5-s simultaneous activation of the infusion pump and inactivation of cue- and hole-lamps. During the remaining timeout period, responses in the active hole had no consequences. Throughout the session, responses in the inactive hole had no programmed consequences but were recorded by the software MED-PC for Windows. In order to facilitate METH self-administration, food was not available in the chambers during the daily sessions. METH self-administration was continued until the deviations

were less than 15% of the mean of active responses on 3 consecutive training days. At the end of the METH self-administration training phase, 32 mice of the METH self-administration group demonstrated a clear ability to discriminate active from inactive responses and then were subjected to extinction training. The other 18 mice were excluded from the analysis of METH self-administration data since the mice could not acquire stable METH self-administration because of a failure of catheter patency.

2.6. Extinction training

The extinction training conditions were the same for all groups of mice ($n=32$) in both cue-induced and drug-primed reinstatement of METH-seeking behavior. During the extinction phase, the syringe was removed from the infusion pump and METH was unavailable. The cue- and hole-lamps were not presented during these sessions. Accordingly, the nose-poking responses in the previous active hole were disassociated from METH infusion. The house light was on throughout extinction sessions. Nose-poking responses in the previous active hole were included in the number of active responses. Nose-poking responses in the previous inactive hole were included in the number of inactive responses. Extinction sessions were conducted daily (6–10 days) until the criterion was met (less than 25 active responses or 30% of active responses in the stable self-administration phase on 2 consecutive days). Accordingly, the mice could not discriminate the active from inactive nose-poking responses when the criteria were achieved in the late phase of extinction training. Two mice could not meet the extinction criterion and were excluded from all the data in this study.

2.7. Cue-induced reinstatement testing

Tests for cue-induced reinstatement were conducted under the conditions used in the extinction sessions but with METH-paired cue- and hole-lamps. Following the last extinction session, mice ($n=16$) were separated into two groups. One group of mice (no relapse (No-RLP) group, $n=8$) was subjected to an additional 3-h extinction session (without METH and METH-paired cue- and hole-lamps), whereas the other group of mice (cue-induced relapse (Cue-RLP) group, $n=8$) was subjected to a 3-h cue-induced reinstatement testing session. During the cue-induced reinstatement session, cue- and hole-lamps were on, which indicated the availability of METH during the self-administration phase. However, METH was unavailable after mice made active nose-poking responses under the same schedule of reinforcement as that in the self-administration phase. Nose-poking responses in previously active holes and inactive holes were recorded by the software MED-PC for Windows, respectively. Throughout the cue-induced reinstatement session, the house light was on.

2.8. METH-primed reinstatement testing

Following the last extinction session, mice ($n=14$) were separated into three groups. Two groups of mice ($n=4$ for each group) were subjected to i.p. METH-primed reinstatement testing at doses of 0.5 mg/kg and 1.0 mg/kg METH. Another group of mice ($n=6$) was subjected to both i.v. METH injection (0.2 mg/kg) and self-injected METH (0.5 mg/kg) primed reinstatement testing. For i.p. METH-primed reinstatement testing, mice were placed into the operant chamber and subjected to a 3-h test session immediately after 0.5 mg/kg or 1.0 mg/kg of METH was administered intraperitoneally. During the test session, conditions in the test chamber were the same as those in extinction sessions. For reinstatement induced by both i.v. injection of METH and self-injected METH primed reinstatement, mice were first administered 0.2 mg/kg of METH intravenously via the catheter, then immediately placed into the operant conditioning chamber for METH self-administration in the absence of cue- and hole-lamps (house light was on) until they self-administered 0.5 mg/kg of METH (total METH intake, including passive and active intake, 0.7 mg/kg) within 1 h. Subsequently, mice were subjected to a 3-h test session, in which the drug-primed reinstatement of METH-seeking behavior was controlled by the computer program used in the extinction phase in the absence of both METH infusion and predictive cue- and hole-lamps but with the house light on throughout the test session.

2.9. Data analysis

All data were expressed as the mean ± S.E. For statistical analyses, a repeated two-way measure of variance (ANOVA) was performed for the nose-poking responses during the self-administration and the subsequent extinction training phase, followed post hoc by the Bonferroni/Dunn test. The other data in our study were examined with the one-way ANOVA, followed post hoc by the Bonferroni/Dunn test. In all cases, a significant difference was set at $P<0.05$.

3. Results

3.1. Saline or METH self-administration and extinction training

After the same number of sessions of self-administration under an FR1/FR2 schedule of reinforcement (FR1 on day 1–4 and FR2 on day 5–10), mice in the saline group (Fig. 1A) could not discriminate active from inactive nose-poking responses. By contrast, mice in the METH self-administration group could gradually discriminate active from inactive nose-poking responses (Fig. 1B, a repeated measure two-way ANOVA, $F_{(2,599)}=222.35$, $P<0.001$), suggesting that the increase in active nose-poking responses in the METH self-administration group of mice depended on the METH reinforcement. Then, mice exhibited stable active nose-poking response rates during the late phase of METH self-administration with a within-subject variability of less than 15% in daily active nose-poking responses for at least 3 consecutive days. The mean number of active nose-poking responses to METH reinforcement during the stable phases of self-administration was 58.7 ± 2.9 in a daily 3-h session. The average amount of METH taken by mice of the METH self-administration group ($n=30$) during a daily 3-h session was 1.89 ± 0.12 mg/kg.

Following the stable responses to METH self-administration, the mice were then subjected to daily 3-h sessions of extinction training. The data in Fig. 1C demonstrate the operant conditioning behavior in the first 2 days and the last 4 days during the extinction training phase. The subsequent daily 3-h sessions of extinction training resulted in a gradual decrease in active nose-poking responses. After 6–10 daily 3-h sessions of extinction training, almost all the mice met the extinction criterion (less than 25 active responses or 30% of active responses in the stable self-administration phase during a daily 3-h session on 2 consecutive days). The data for two mice obtained during the self-administration, extinction and reinstatement phases were excluded since the mice could not meet the extinction criterion after 10 sessions of extinction training. On the last day of the extinction phase, the average number of active nose-poking responses (16.1 ± 3.2) was significantly small as compared with that (80.4 ± 4.9) on the first day of the extinction phase (Fig. 1C, a one-way ANOVA, followed post hoc by the Bonferroni/Dunn test, $P<0.001$) and that (59.4 ± 3.0) on the last day of self-administration (Fig. 1B and C, a one-way ANOVA, followed post hoc by the Bonferroni/Dunn test, $P<0.001$). During the last two sessions of the extinction, the mice could not discriminate the active (e.g. 16.1 ± 3.0 for the last session) from the inactive (13.8 ± 5.6 for the last session) nose-poking responses, whereas the mice could discriminate the

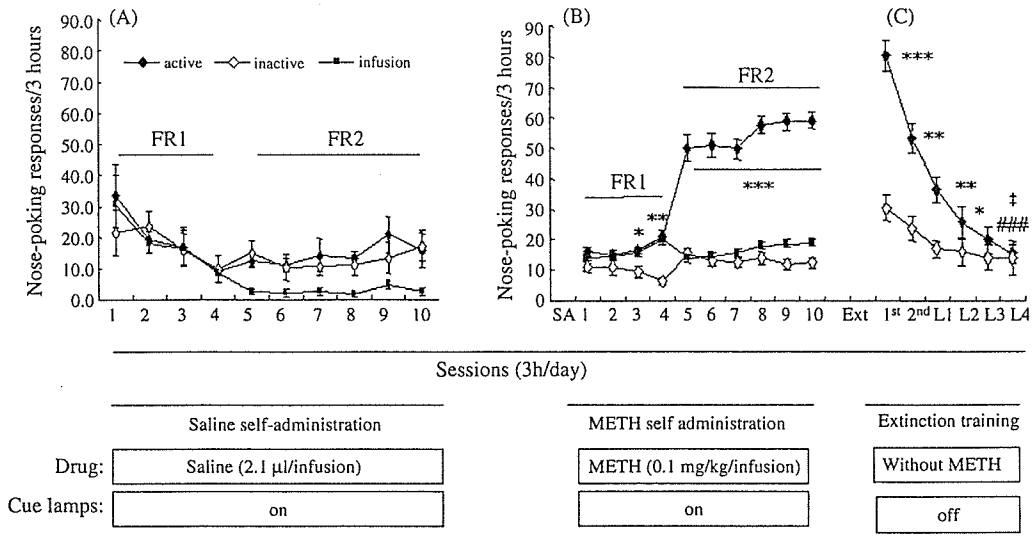

Fig. 1. Nose-poking responses during saline self-administration in the saline group ($n=5$), and METH self-administration and the extinction training phase in the reinstatement group ($n=30$). (A) Active, inactive, nose-poking responses and the number of infusions during 10 daily 3-h sessions of saline self-administration in the saline group. (B) Active, inactive, nose-poking responses and the number of infusion during METH self-administration in the reinstatement group. (C) Active and inactive nose-poking responses during extinction training in the reinstatement group. The data were from the first 2 daily 3-h sessions (indicated by 1st and 2nd) and the last 4 daily 3-h sessions (indicated by L1, L2, L3 and L4, respectively) during 6–10 extinction training sessions. Data are presented as the mean ± S.E. $^{*}P<0.05$, $^{**}P<0.01$, $^{***}P<0.001$ active vs. inactive nose-poking responses during METH self-administration and extinction (a repeated two-way measure of variance (ANOVA), followed post hoc by the Bonferroni/Dunn test). $^{\#\#\#}P<0.001$ vs. active nose-poking responses on the last day of the self-administration phase. $^{\ddagger}P<0.001$ vs. active nose-poking responses on the first day of extinction training (a one-way ANOVA, followed post hoc by the Bonferroni/Dunn test).

active (80.4 ± 4.9) from the inactive (30.6 ± 4.5) nose-poking responses in the first session of extinction training. These data suggested that the METH-paired active nose-poking responses were extinguished after 6–10 sessions of extinction training.

3.2. Cue-induced reinstatement of METH-seeking behavior

After meeting the extinction criterion, mice ($n=16$) were separated into two groups. The No-RLP group of mice ($n=8$) were subjected to an additional 3-h session of extinction training on the following day. As shown in Fig. 2, the mice in this group showed similar nose-poking responses to those in the last day of the extinction training phase, which were significantly lower than those in the last day of the METH self-administration phase (a one-way ANOVA followed post hoc by the Bonferroni/Dunn test, $P<0.001$). On the following day, after exposure to both cue- and hole-lamps as in the METH self-administration phase, the Cue-RLP group of mice ($n=8$) made a significantly larger number of active nose-poking responses (a one-way ANOVA, followed post hoc by the Bonferroni/Dunn test, $P<0.001$) than the No-RLP group of mice although METH was not delivered. However, there was no difference in inactive nose-poking responses between the Cue-RLP and the No-RLP group, suggesting that contingent cues could reliably reinstate METH-seeking behavior in the Cue-RLP group of mice. During the reinstatement period, the Cue-RLP group of mice could also discriminate the active responses, previously associated with METH infusion, from the inactive nose-poking responses (a one-way ANOVA, followed post hoc by the Bonferroni/Dunn test, $P<0.001$).

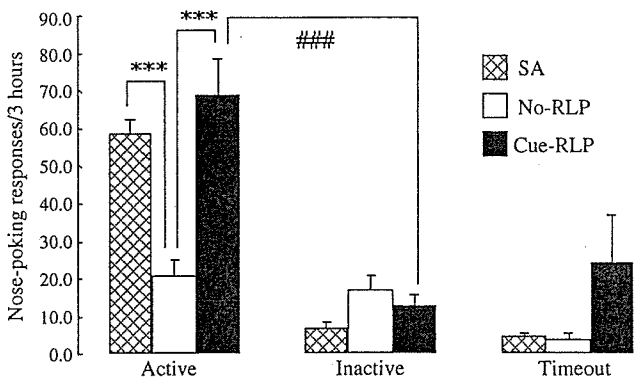

Fig. 2. Nose-poking responses in all groups of mice during METH self-administration (SA, $n=16$), in the control group of mice (No-RLP, without cue- and hole-lamps and METH infusion, $n=8$) and in the cue-induced reinstatement group (Cue-RLP, $n=8$). Data are presented as the mean ± S.E. $^{***}P<0.001$ vs. active nose-poking in the No-RLP group. $^{\#\#\#}P<0.001$ vs. inactive nose-poking responses in the Cue-RLP group. Statistical analysis was conducted with a one-way ANOVA, followed post hoc by the Bonferroni/Dunn test. RLP: relapse.

3.3. METH-primed reinstatement of drug-seeking behavior

After meeting the extinction criterion, mice ($n=14$) were separated into three groups. Two groups of mice ($n=4$ for each group) were subjected to an additional 3-h session of i.p. priming-induced reinstatement testing immediately after the i.p. priming injection of METH (0.5 mg/kg or 1.0 mg/kg) on the following day. Compared with active nose-poking responses on the last day of the extinction training phase (extinction group, $n=14$), two i.p. priming groups of mice (Fig. 3) failed to show reinstatement of METH-paired active nose-poking responses, respectively, at 0.5 mg/kg or 1.0 mg/kg of METH. Another group of mice ($n=6$), on the following day, were firstly administered 0.2 mg/kg of METH via the catheter, then immediately placed

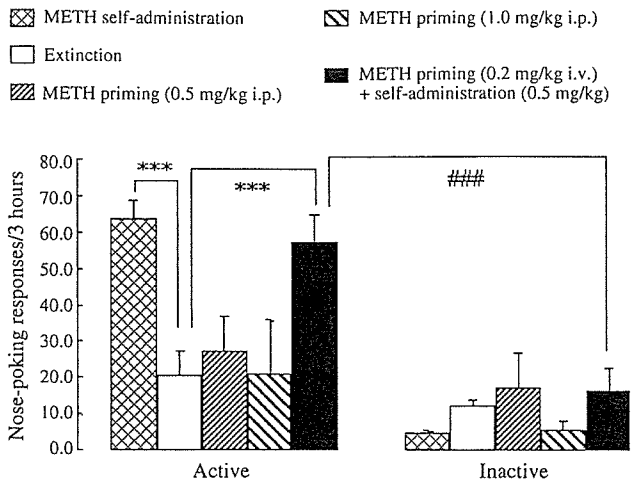

Fig. 3. Nose-poking responses in all groups of mice during METH self-administration (SA, $n = 14$), on the last day of extinction training (extinction group, $n = 14$) and in different subgroups during the METH-primed reinstatement test. Data are presented as the mean ± S.E. $^{***}P < 0.001$ vs. active nose-poking responses in the last session of extinction. $^{###}P < 0.001$ vs. inactive nose-poking responses during the METH-primed reinstatement test. Statistical analysis was conducted with a one-way ANOVA, followed post hoc by the Bonferroni/Dunn test.

into the chamber for self-administration (without METH-paired cue- and hole-lamps) until 0.5 mg/kg of METH was earned within 1 h. Subsequently, the reinstatement was measured in the mice for an additional 3-h session, in which METH was unavailable and without METH-paired cue- and hole-lamps. The mice in this group demonstrated more active nose-poking responses (Fig. 3, a one-way ANOVA followed post hoc by the Bonferroni/Dunn test, $P < 0.001$) compared with active nose-poking responses on the last day of the extinction training phase (extinction group). The mice could also discriminate active from inactive nose-poking responses during reinstatement testing (Fig. 3, a one-way ANOVA followed post hoc by the Bonferroni/Dunn test, $P < 0.001$).

4. Discussion

A new procedure for reinstating extinguished METH-seeking behavior in mice was established in the present study. Two groups of researchers have already reported similar procedures using cocaine in mice [20,26]. However, no further investigation based on their reinstatement procedures has been published to date. Compared with the previous procedures, the present procedure has the following advantages. First, a nose-poking response task was introduced instead of the more difficult lever-pressing response task. Lever-pressing is hard by mice, since the task is complicated for them and their muscle is not strong enough to press the lever in relation to reinforcement. Body weight of mice for experiments (8-week-old) usually is 20–30 g. Therefore, it seems to take longer time for mice to acquire lever-pressing responses. On the contrary, nose-poking task is very easy for mice, since the mice have an inherent ability to do nose-poking responses. The introduction of the nose-poking task might be useful to facilitate the acquisition of METH self-administration. Second, instead of a single fixed ratio 1 (FR1) schedule of cocaine self-administration, an FR1/FR2 schedule of METH reinforcement was taken into the late phase of self-administration. Thus, it seemed to be easier for researchers to examine whether the mice depended on METH-taking during self-administration and whether METH-paired active nose-poking responses were extinguished after extinction training. Mice would exhibit many more active than inactive nose-poking responses if they had already depended on METH-taking. In contrast, mice would emit similar numbers of active and inactive nose-poking responses if they have already been extinguished of METH-seeking behavior. Third, the present reinstatement procedure under an FR1/FR2 schedule seemed to be useful to shorten the duration (6–10 days in our study) of the extinction training phase. In the present experiment, only two mice were excluded since they could not meet the extinction criterion (less than 25 active responses or 30% of active responses at the stable self-administration phase during a daily 3-h session on 2 consecutive days) after 10 sessions of extinction training. In contrast, Fuchs et al. have shown that mice are considerably resistant to extinction (18.3 ± 2.7 days) to reach a similar criterion (less than 25 active responses in a 2-h test session), although it could not be excluded that the different extinction duration between cocaine-conditioned lever-press responses and METH-conditioned nose-poking responses in mice results from different mechanisms between cocaine- and METH-conditioning effects. Together, the present procedure for the METH self-administration, extinction and cue-induced reinstatement is a feasible, even useful, mouse model of drug-seeking behavior with which to identify target genes involved in the relapse of drug dependence, since there is only one limitation for developing intravenous self-administration and the subsequent reinstatement of drug seeking in mice, which is the relatively short duration of jugular catheter patency. However, it remained unclear in the present study whether the new reinstatement procedure could be extended to other drugs of abuse such as nicotine or other inbred strains of mice such as 129 × 1/SvJ mice.

Consistent with previous studies using cocaine in 129 × 1/SvJ and C57BL/6 mice [20,26], exposure to METH-paired cues, in the present study, reliably triggered a relapse of extinguished METH-seeking behavior in C57BL/6J mice, and an i.p. priming injection of METH at the doses examined in this study failed to reinstate drug-seeking behavior in C57BL/6J mice although similar doses of i.p. METH priming reliably provoked the reinstatement of extinguished METH-seeking behavior in rats [1]. These findings suggested that the reinstatement procedure in determining extinguished cocaine-seeking behavior in C57BL/6J and 129 × 1/SvJ mice could be extended to other drugs of abuse such as METH in the present study. However, failure of the i.p. priming injection of cocaine to reinstate drug-seeking behavior has been demonstrated once again in the present study by using METH in C57BL/6J mice. Although it was postulated that C57BL/6J would demonstrate similar or lower sensitivity to the priming effect of cocaine than 129 × v1/SvJ mice [26], Fuchs et al. demonstrated clearly that wide range of cocaine doses (1–40 mg/kg, i.p.) did not reinstate cocaine-seeking behavior in C57BL/6 mice whereas Highfield et al. showed that 6 mg/kg of i.v. cocaine priming modestly rein-

stated cocaine-seeking behavior in 129 × 1/SvJ mice. Together with previous studies in rats, these findings indicate at least two possibilities. First, mice may be much more sensitive than rats to differences in the subjective effects of i.v. versus i.p. cocaine during self-administration training and reinstatement testing, thus leading to a failure of i.p. cocaine primed reinstatement in mice. Second, the reinstatement procedure itself (e.g. the short duration of extinction training, and the same day for the extinction training and the following reinstatement testing in the report from Highfield et al.) may play an important role in drug-primed reinstatement of extinguished drug-seeking behavior in mice. In our pilot studies, however, an i.v. primed injection of METH (0.2 mg/kg or 0.8 mg/kg) via the catheter also failed to reinstate METH-seeking behavior (data not showed). Therefore, we further tried to develop new procedure for METH-primed reinstatement by using a combination of i.v. injection and self-injected METH under the same self-administration, extinction schedule as METH-paired cue-induced reinstatement test. Such a combination successfully increased the reinstatement of METH-seeking behavior. Some may make the following points regarding this combination-primed reinstatement procedure. First, such a combination of priming could not exactly distinguish the reinstatement induced by passive METH-priming (i.p. priming injection) from that induced by active METH-priming (self-injection of METH). Second, the METH primed reinstatement might reflect an acute extinction behavior immediately after the cessation of the 1-h METH self-injection experience. Third, such METH-primed reinstatement might just demonstrate re-self-administration behavior after 6–10 sessions of extinction training. However, any possibility mentioned above, to some extent, might reflect relapse behavior in humans [17,29,42,43,45]. In some sense, such a combination-primed reinstatement procedure may be one way to investigate specific gene functions in drug-primed relapse until a more optimal drug-primed reinstatement procedure is established in mice.

In conclusion, the present findings suggested that the cue-induced and drug-primed reinstatement of extinguished METH-seeking behavior in the new procedure was a feasible way to identify genes involved in the relapse of drug-seeking behavior in genetically modified mouse strains and the mechanism of action of drugs of abuse. The introduction of a natural nose-poking response system and an FR1/FR2 schedule of reinforcement might shorten the duration of self-administration and extinction training phase, thus ameliorating the effectiveness of the procedure to reinstate extinguished drug-seeking behavior in mice. However, a more practical way to achieve drug-primed reinstatement in mice remains to be established.

Acknowledgements

This study was supported in part by a Grant-in-aid for Scientific Research and Special Coordination Funds for Promoting Science and Technology, the Target-Oriented Brain Science Research Program, from the Ministry of Education, Culture, Sports, Science and Technology of Japan; by a Grant-in-aid for Health Science Research on Regulatory Science of Pharmaceuticals and Medical Devices, and Dementia and Fracture from the Ministry of Health, Labor and Welfare of Japan; by the Japan Society for the Promotion Science Joint Research Project under the Japan–Korea Basic Scientific Cooperation Program; by a Smoking Research Foundation Grant for Biomedical Research; by a Grant-in-aid for Scientific Research (B) and Young Scientists (A); by an Uehara Memorial Foundation Research Fellowship; and in part by the 21st Century Center of Excellence Program "Integrated Molecular Medicine for Neuronal and Neoplastic Disorders" from the Ministry of Education, Culture, Sports, Science and Technology of Japan.

References

[1] Anggadiredja K, Nakamichi M, Hiranita T, Tanaka H, Shoyama Y, Watanabe S, et al. Endocannabinoid system modulates relapse to methamphetamine seeking: possible mediation by the arachidonic acid cascade. Neuropsychopharmacology 2004;29:1470–8.

[2] Anglin MD, Burke C, Perrochet B, Stamper E, Dawud-Noursi S. History of the methamphetamine problem. J Psychoactive Drugs 2000;32:137–41.

[3] Bonson KR, Grant SJ, Contoreggi CS, Links JM, Metcalfe J, Weyl HL, et al. Neural systems and cue-induced cocaine craving. Neuropsychopharmacology 2002;26:376–86.

[4] Bowers MS, McFarland K, Lake RW, Peterson YK, Lapish CC, Gregory ML, et al. Activator of G protein signaling 3: a gatekeeper of cocaine sensitization and drug seeking. Neuron 2004;42:269–81.

[5] Caine SB, Negus SS, Mello NK, Patel S, Bristow L, Kulagowski J, et al. Role of dopamine D2-like receptors in cocaine self-administration: studies with D2 receptor mutant mice and novel D2 receptor antagonists. J Neurosci 2002;22:2977–88.

[6] Carney JM, Landrum RW, Cheng MS, Seale TW. Establishment of chronic intravenous drug self-administration in the C57BL/6J mouse. Neuroreport 1991;2:477–80.

[7] Carroll ME, Comer SD. Animal models of relapse. Exp Clin Psychopharmacol 1996;4:11–8.

[8] Chiamulera C, Epping-Jordan MP, Zocchi A, Marcon C, Cottiny C, Tacconi S, et al. Reinforcing and locomotor stimulant effects of cocaine are absent in mGluR5 null mutant mice. Nat Neurosci 2001;4:873–4.

[9] Cohen JB, Dickow A, Horner K, Zweben JE, Balabis J, Vandersloot D, et al. Methamphetamine treatment project: abuse and violence history of men and women in treatment for methamphetamine dependence. Am J Addict 2003;12:377–85.

[10] Comings DE, Muhleman D, Ahn C, Gysin R, Flanagan SD. The dopamine D2 receptor gene: a genetic risk factor in substance abuse. Drug Alcohol Depend 1994;34:175–80.

[11] Cossu G, Ledent C, Fattore L, Imperato A, Bohme GA, Parmentier M, et al. Cannabinoid CB1 receptor knockout mice fail to self-administer morphine but not other drugs of abuse. Behav Brain Res 2001;118:61–5.

[12] Crabbe JC, Phillips TJ, Buck KJ, Cunningham CL, Belknap JK. Identifying genes for alcohol and drug sensitivity: recent progress and future directions. Trends Neurosci 1999;22:173–9.

[13] Deroche-Gamonet V, Belin D, Piazza PV. Evidence for addiction-like behavior in the rat. Science 2004;305:1014–7.

[14] Di Ciano P, Everitt BJ. Conditioned reinforcing properties of stimuli paired with self-administered cocaine, heroin or sucrose: implications for the persistence of addictive behaviour. Neuropharmacology 2004;47:202–13.

[15] Ehrman RN, Robbins SJ, Childress AR, O'Brien CP. Conditioned responses to cocaine-related stimuli in cocaine abuse patients. Psychopharmacology 1992;107:523–9.

[16] Elmer GI, Pieper JO, Rubinstein M, Low MJ, Grandy DK, Wise RA. Failure of intravenous morphine to serve as an effective instrumental reinforcer in dopamine D2 receptor knock-out mice. J Neurosci 2002;22:1–6.